Analysis of Single Pile by the Program *GEO Tools*

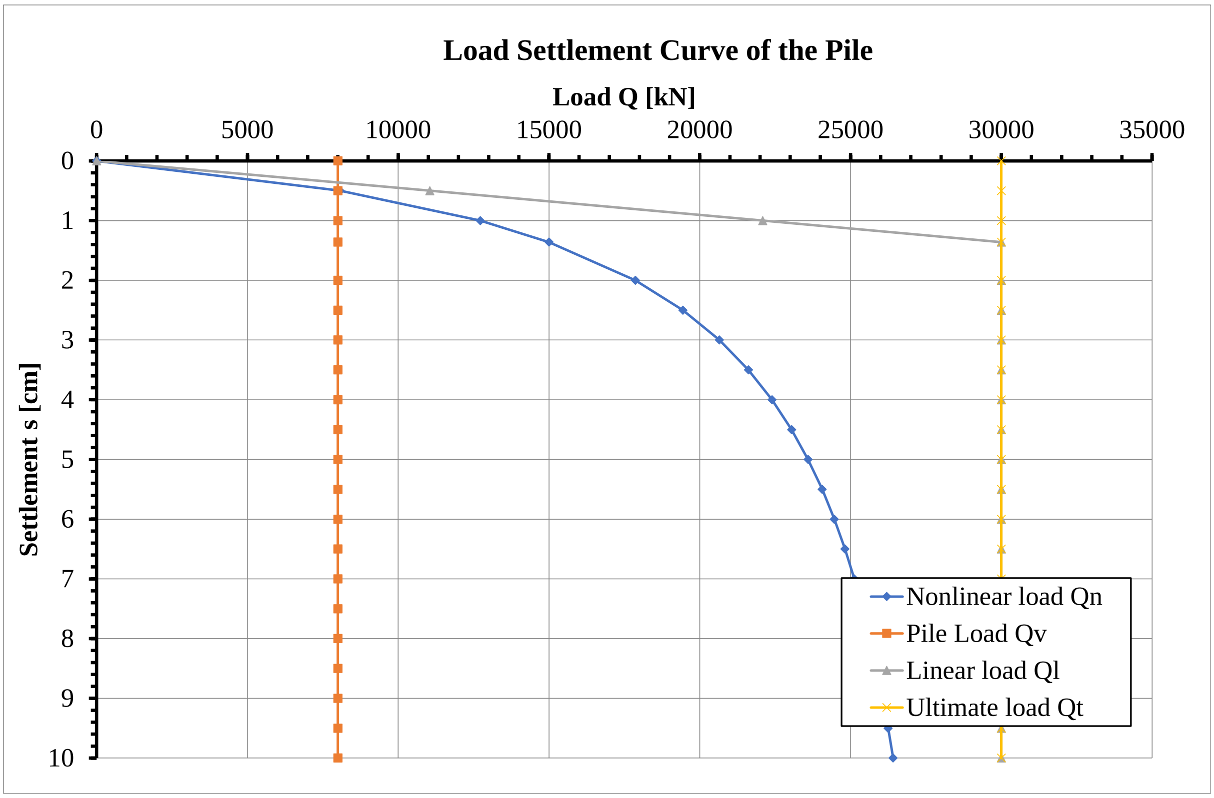

Mahmoud El Gendy
Mohamed El Gendy

Tele.:+1(587) 332-3323
geotec@geotecsoftware.com
www.geotecsoftware.com

2022

Table of Contents

Page

1 Analysis of Single Pile

1.1 Preface

Various problems in geotechnical Engineering can be investigated by the program *GEO Tools*. The original version of *GEO Tools* in *GEOTEC Office* was developed by Prof. *M. Kany*, Prof. *M. El Gendy* (1), and Dr. *A. El Gendy*. After the death of Prof. *Kany*, Prof. *M. El Gendy* and Dr. *A. El Gendy* further developed the program to meet the needs of the practice.

This book describes the procedures and methods available in *GEO Tools* to analyze the single pile. The methods consider various analysis aspects of the single pile such as linear analysis, nonlinear analysis, half-space soil, and multi-layered soil.

GEO Tools has been developed for analyzing the single pile using:

- *Rigid analysis*
- *Elastic analysis*

Many tested examples are presented to verify and illustrate the available methods.

1.2 Determining settlement in soil

In 1936 Raymond *Mindlin* [13] presented a mathematical solution for determining stresses and displacements in soil due to a point load acting beneath the surface of the semi-infinite mass. The following paragraphs illustrate the essential equations to obtain the settlement (displacements) in soil due to loads acting beneath the surface of the semi-infinite mass. The derivation of equations depends on *Mindlin's* solution. These equations are often employed in the numerical analysis of piled foundations. They may have other Geotechnical Engineering applications, such as studying the interaction between foundations and ground anchors or buried structures.

1.2.1 Displacement due to a concentrated load

The displacement w_i [m] at point i due to a concentrated load P_j [kN] acting at point j beneath the surface of a semi-infinite mass, Figure 1.1, according to *Mindlin's* solution can be expressed as:

$$w_i = f_{ij}\, P_j \tag{1.1}$$

where f_{ij} is given by *Mindlin's* solution as:

$$\begin{aligned} f_{ij} = \frac{1}{16\,\pi\, G_s\,(1-\nu_s)} \Bigg(& \frac{3-4\,\nu_s}{R_1} + \frac{8\,(1-\nu_s)^2 - (3-4\,\nu_s)}{R_2} \\ & + \frac{(z-c)^2}{R_1^3} + \frac{(3-4\,\nu_s)\,(z+c)^2 - 2c\,z}{R_2^3} + \frac{6\,c\,z\,(z+c)^2}{R_2^5} \Bigg) \end{aligned} \tag{1.2}$$

where:

$R_1 = \sqrt{r^2 + (z-c)^2}$, $R_2 = \sqrt{r^2 + (z+c)^2}$ and

- c Depth of the point load P_j [kN] from the surface, [m].
- z Depth of the studied point i from the surface, [m].
- r Radial distance between points i and j, [m].
- z-c Vertical distance between points i and j, [m].
- z+c Vertical distance between points i and k, [m].
- f_{ij} Displacement factor of point i due to a unit load at point j, [m/kN].
- G_s Shear modulus of the soil, [kN/m^2], $G_s = \dfrac{E_s}{2\,(1+\nu_s)}$.
- E_s Modulus of elasticity of the soil, [kN/m^2].
- ν_s *Poisson's* ratio of the soil, [-].

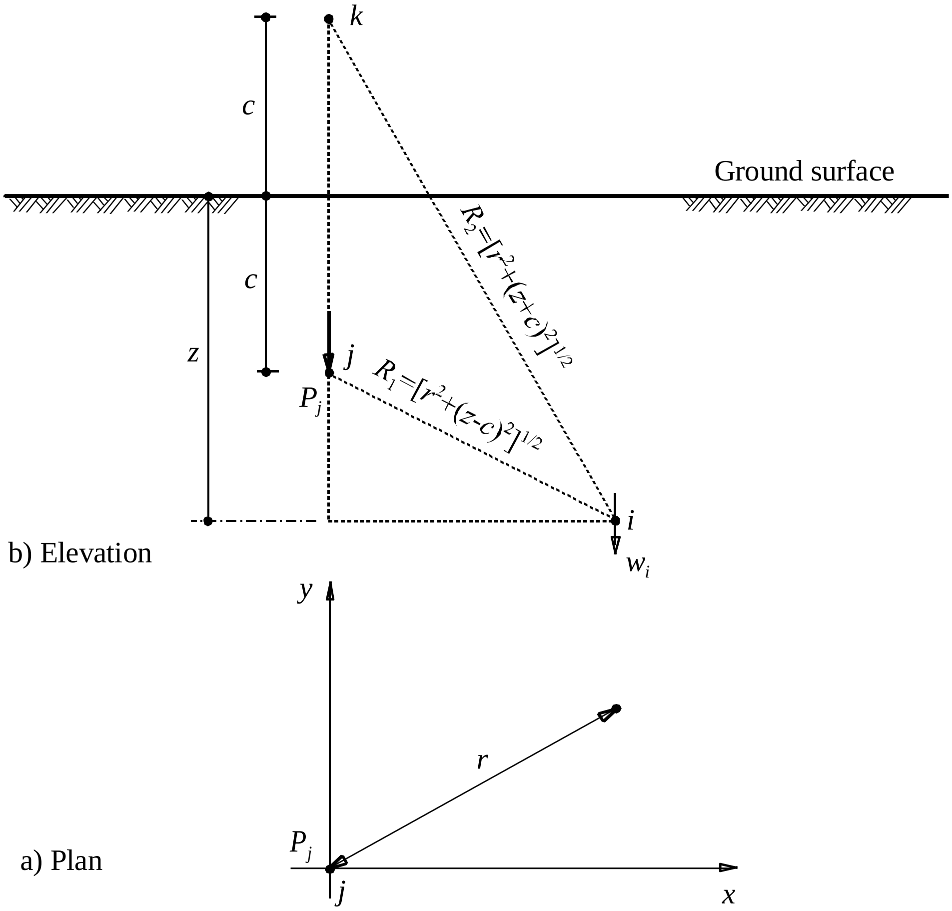

Figure 1.1 Geometry of *Mindlin's* problem.

1.2.2 Displacement at the center due to a circular uniform load

The displacement w_i [m] at the center i of a circular loaded area of radius r_o [m] and a uniform load q [kN/m^2] beneath the surface of a semi-infinite mass, Figure 1.2, can be obtained from:

$$w_i = q\int_0^{2\pi}\int_0^{r_o} f_{ij}\, r\, dr\, d\theta \tag{1.3}$$

Substituting Eq. (1.2) into Eq. (1.3) and carrying out the integration, yields to:

$$\begin{aligned} w_i = \frac{q}{8\,G_s\,(1-\nu_s)}\Bigg(& (3-4\nu_s)\left[\sqrt{r_o^2+(z-c)^2}-\|z-c\|\right] \\ & +\left[8\,(1-\nu_s)^2-(3-4\nu_s)\right]\left[\sqrt{r_o^2+(z+c)^2}-(z+c)\right] \\ & +(z-c)^2\left[\frac{1}{\|z-c\|}-\frac{1}{\sqrt{r_o^2+(z-c)^2}}\right]+\left[(3-4\nu_s)\,(z+c)^2-2\,c\,z\right]\left[\frac{1}{z+c}-\frac{1}{\sqrt{r_o^2+(z+c)^2}}\right] \\ & +2\,c\,z\,(z+c)^2\left[\frac{1}{(z+c)^3}-\frac{1}{\left(r_o^2+(z+c)^2\right)^{3/2}}\right]\Bigg) \end{aligned} \tag{1.4}$$

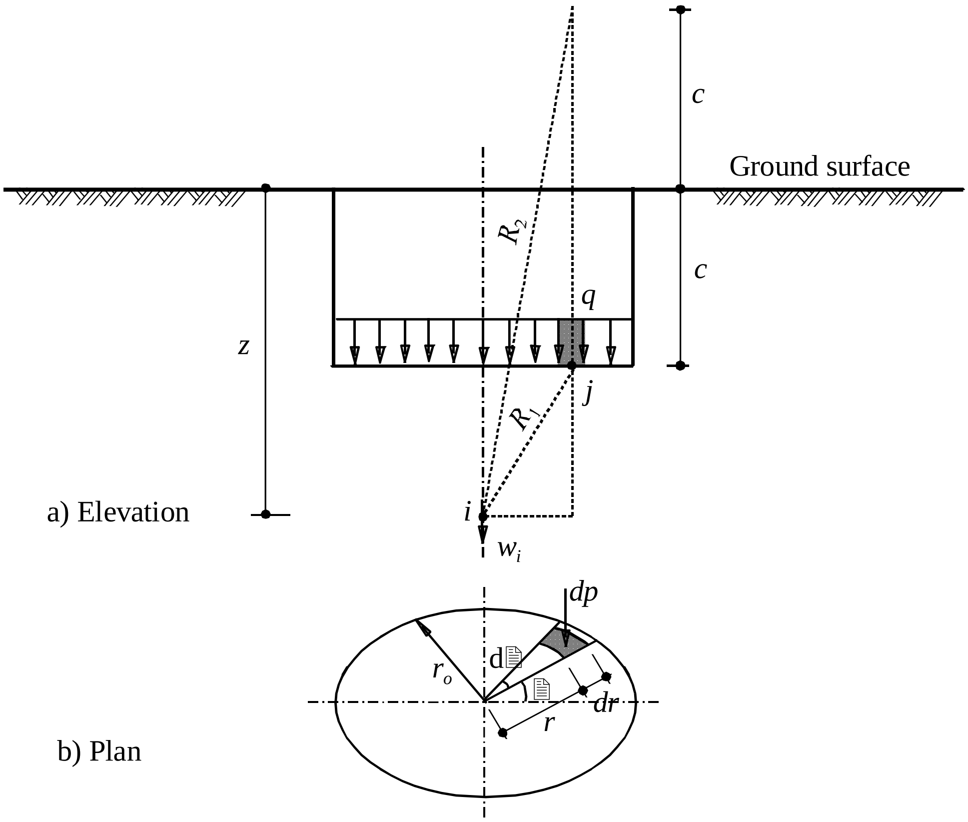

Figure 1.2 Geometry of circular loaded area for finding displacement at center.

At depth $z = c$, the displacement at the center of a circularly loaded area is given by:

$$w_i = \frac{q}{8\,G_s\,(1-\nu_s)}\left((3-4\,\nu_s)\,r_o + \left[8\,(1-\nu_s)^2 - (3-4\,\nu_s)\right]\left[\sqrt{r_o^2+4\,z^2} - 2\,z\right] \right.$$
$$\left. + \left[4\,z^2\,(3-4\,\nu_s) - 2\,z^2\right]\left[\frac{1}{2\,z} - \frac{1}{\sqrt{r_o^2+4\,z^2}}\right] + \left[1 - \frac{8\,z^4}{\left(r_o^2+4\,z^2\right)^{3/2}}\right]\right) \tag{1.5}$$

1.2.3 Displacement at the edge due to a circular uniform load

The displacement w_i [m] at the edge i of a circularly loaded area of radius r_o [m] and a uniform load q [kN/m^2] beneath the surface of a semi-infinite mass, Figure 1.3, can be obtained from:

$$w_i = 2\,q\int_0^{\frac{\pi}{2}} \int_0^{2\,r_0\cos\theta} f_{ij}\, r\, dr\, d\theta \tag{1.6}$$

The integral with respect to r in the above equation can be carried out analytically, while that with respect to θ is evaluated numerically. This is because the first integration will contain terms with complete elliptic integrals, which cannot be integrated into a closed-form. Substituting Eq. (1.2) into Eq. (1.6) and carrying out the integration with respect to r leads to:

$$w_i = I_r + I_\theta \tag{1.7}$$

where terms I_r and I_θ are given by:

$$I_r = \frac{q}{16\,G_s\,(1-\nu_s)}\left(\frac{2\,c\,z\,(z+c)^2}{(z+c)^3} - \left[8(1-\nu_s)^2 - (3-4\,\nu_s)\right](z+c)]\right.$$
$$\left. -\,(2-4\,\nu_s)\left\|z-c\right\| + \frac{(3-4\,\nu_s)\,(z+c)^2 - 2\,c\,z}{z+c}\right) \tag{1.8}$$

$$I_\theta = \frac{q}{8\,\pi\,G_s\,(1-\nu_s)}\int_0^{\frac{\pi}{2}}\left((3-4\,\nu_s)\left[\sqrt{4\,r_o^2\cos^2\theta + (z-c)^2}\right]\right.$$
$$+\left[8\,(1-\nu_s)^2 - (3-4\,\nu_s)\right]\left[\sqrt{4\,r_o^2\cos^2\theta + (z+c)^2}\right]$$
$$-\frac{(z-c)^2}{\sqrt{4\,r_o^2\cos^2\theta + (z-c)^2}} - \frac{(3-4\,\nu_s)\,(z+c)^2 - 2\,c\,z}{\sqrt{4\,r_o^2\cos^2\theta + (z+c)^2}} \tag{1.9}$$
$$\left. -\frac{2\,c\,z\,(z+c)^2}{\left(4\,r_o^2\cos^2\theta + (z+c)^2\right)^{3/2}}\right)d\,\theta$$

The integral I_θ may be evaluated numerically using *Simpson's* rule. In performing the numerical integration, intervals of $\pi/50$ in θ were adequate according to *Poulos*/ *Davis* (1968) [16].

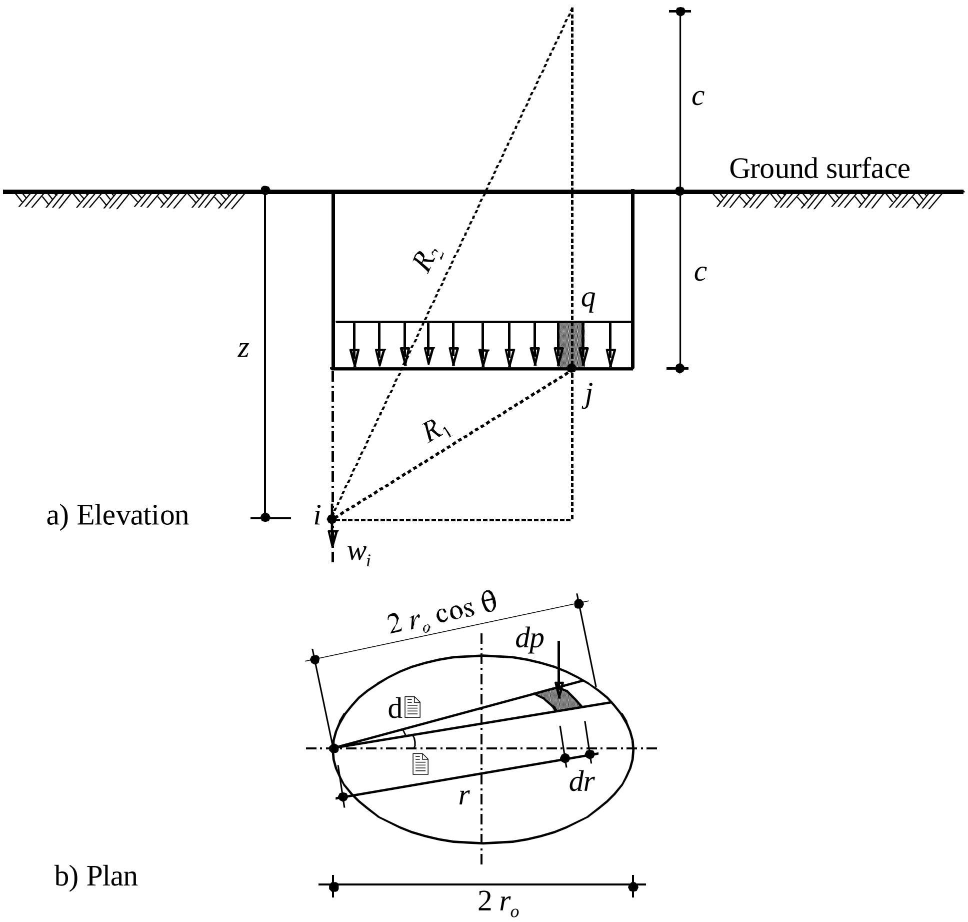

Figure 1.3 Geometry of circular loaded area for finding the displacement at edge.

1.2.4 Displacement due to a line load

The displacement w_i [m] at the point i due to a line load T [kN/m] beneath the surface of a semi-infinite mass, Figure 1.4, can be obtained from:

$$w_i = T \int_{l_1}^{l_2} f_{ij}\, dc \tag{1.10}$$

Substituting Eq. (1.2) into Eq. (1.10) and carrying out the integration, leads to:

$$w_i = \frac{T}{16\pi\ G_s\,(1-\nu_s)}\ \left(I_1 + I_2 + I_3 + I_4 + I_5\right) \tag{1.11}$$

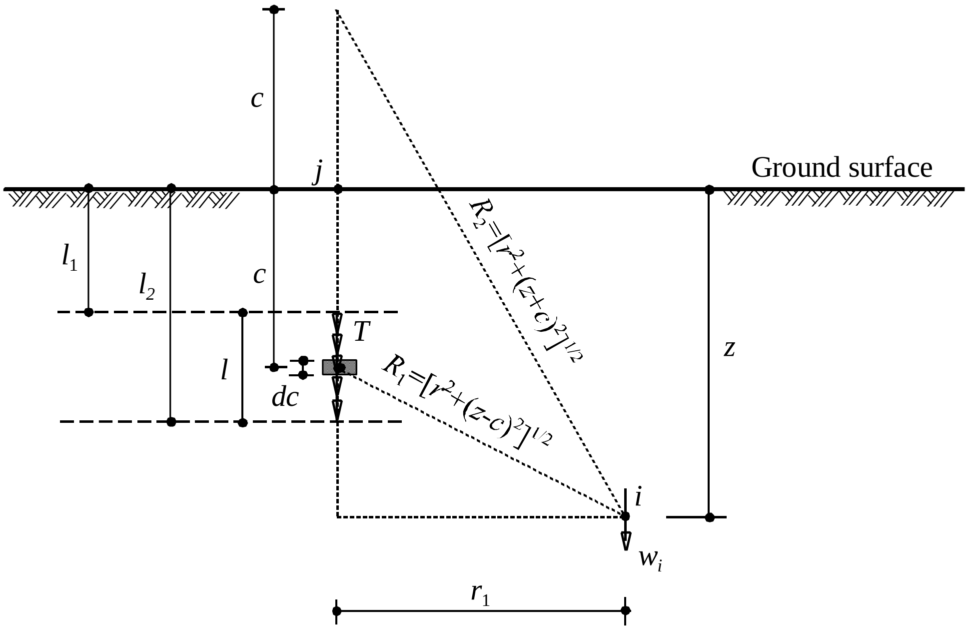

Figure 1.4 Geometry of line load.

1.2.5 Displacement at the center due to a cylindrical surface stress

The displacement w_i [m] at the center i of a cylindrical surface of radius r_o and height l with stress τ [kN/m^2] acting on its surface beneath the surface of a semi-infinite mass, Figure 1.5, can be obtained from:

$$w_i = \tau\, r_o \int_0^{2\pi} \int_{l_1}^{l_2} f_{ij}\, dc\, d\theta \tag{1.12}$$

Substituting Eq. (1.2) into Eq. (1.12) and carrying out the integration, leads to:

$$w_i = \frac{\tau\, r_o}{8\, G_s\,(1-\nu_s)}\ \left(I_1 + I_2 + I_3 + I_4 + I_5\right) \tag{1.13}$$

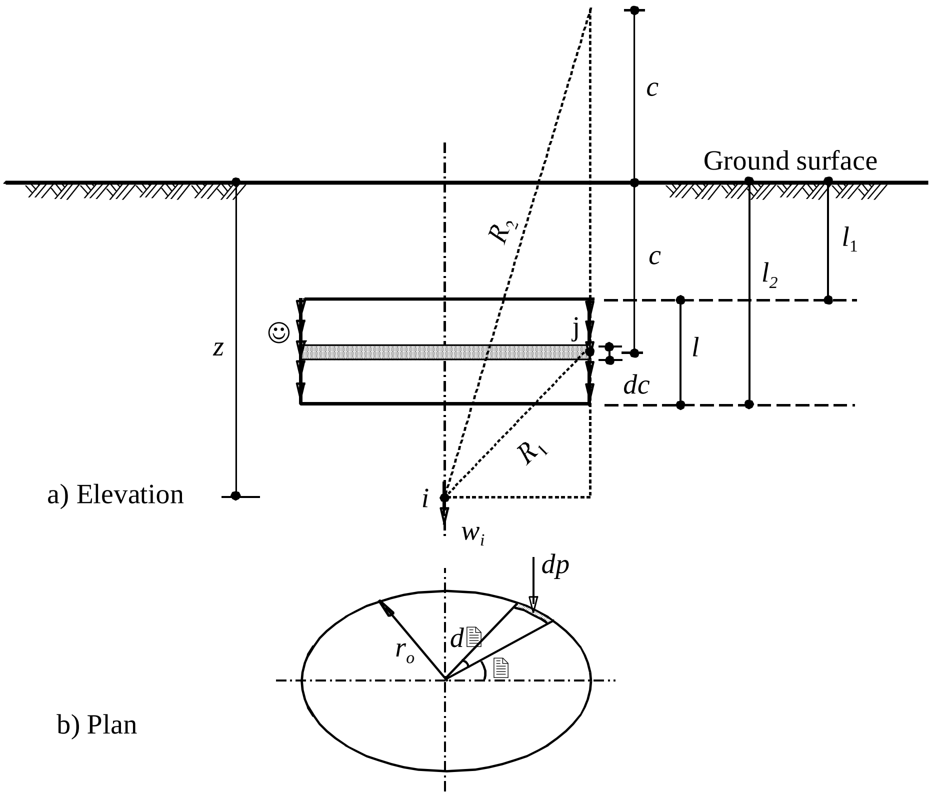

Figure 1.5 Geometry of cylindrical surface stress for finding the displacement at center.

where terms I_1 to I_5 are given by:

$$I_1 = (3 - 4\,\nu_s)\,\ln\left[\frac{\sqrt{r_1^2 + (z - l_2)^2} - (z - l_2)}{\sqrt{r_1^2 + (z - l_1)^2} - (z - l_1)}\right] \tag{1.14}$$

$$I_2 = \left[8\,(1 - \nu_s)^2 - (3 - 4\,\nu_s)\right]\ln\left[\frac{\sqrt{r_1^2 + (z + l_2)^2} + (z + l_2)}{\sqrt{r_1^2 + (z + l_1)^2} + (z + l_1)}\right] \tag{1.15}$$

$$I_3 = \ln\left[\frac{\sqrt{r_1^2 + (z - l_2)^2} - (z - l_2)}{\sqrt{r_1^2 + (z - l_1)^2} - (z - l_1)}\right] + \frac{z - l_2}{\sqrt{r_1^2 + (z - l_2)^2}} - \frac{z - l_1}{\sqrt{r_1^2 + (z - l_1)^2}} \tag{1.16}$$

$$\begin{aligned} I_4 = {} & (3 - 4\,\nu_s)\left(\ln\left[\frac{\sqrt{r_1^2 + (z + l_2)^2} + (z + l_2)}{\sqrt{r_1^2 + (z + l_1)^2} + (z + l_1)}\right] - \frac{(z + l_2)}{\sqrt{r_1^2 + (z + l_2)^2}} + \frac{(z + l_1)}{\sqrt{r_1^2 + (z + l_1)^2}}\right) \\ & - 2\,z\left(\frac{1}{\sqrt{r_1^2 + (z + l_1)^2}} - \frac{1}{\sqrt{r_1^2 + (z + l_2)^2}} + \frac{z\,(z + l_1)}{r_1^2\sqrt{r_1^2 + (z + l_1)^2}} - \frac{z\,(z + l_2)}{r_1^2\sqrt{r_1^2 + (z + l_2)^2}}\right) \end{aligned} \tag{1.17}$$

$$I_5 = \frac{6\,z\left[r_1^4 - z\,(z + l_2)^3\right]}{3\,r_1^2\left[r_1^2 + (z + l_2)^2\right]^{3/2}} - \frac{6\,z\left[r_1^4 + z\,(z + l_1)^3\right]}{3\,r_1^2\left[r_1^2 + (z + l_2)^2\right]^{3/2}} - \frac{6\,z}{\sqrt{r_1^2 + (z + l_2)^2}} + \frac{6\,z}{\sqrt{r_1^2 + (z + l_1)^2}} \tag{1.18}$$

where:

l_1 Start depth of the line load T or the shear stress τ from the surface, [m].

l_2 End depth of the line load T or the shear stress τ from the surface, [m].
l Length of the line load T or the shear stress τ, [m].
r_1 Radial distance between point i and j [m]. $r_1 = r_o$ for shaft load and $r_1 = r$ for line load.

1.2.6 Displacement at the edge due to a cylindrical surface stress

The displacement w_i [m] at the edge i of a cylindrical surface of radius r_o and height l with stress τ [kN/m^2] acting on its surface beneath the surface of a semi-infinite mass, Figure 1.6, can be obtained from:

$$w_i = 4\,\tau\, r_o \int_0^{\frac{\pi}{2}} \int_{l_1}^{l_2} f_{ij}\, dc\, d\theta \tag{1.19}$$

The integral with respect to c in the above equation can be carried out analytically, while that with respect to θ is evaluated numerically. This is because the first integration will contain terms with complete elliptic integrals, which cannot be integrated into a closed-form. Substituting Eq. (1.2) into Eq. (1.19) and carrying out the integration with respect to c leads to:

$$w_i = \frac{\tau\, r_o}{4\,\pi\, G_s (1-\nu_s)} \int_0^{\frac{\pi}{2}} \left(I_1 + I_2 + I_3 + I_4 + I_5 \right) d\theta \tag{1.20}$$

where terms I_1 to I_5 are in Eqns (1.14) to (1.18) with replacing r_1 by $2\, r_o \cos\theta$. Integrals in the above equations may be evaluated numerically using *Simpson's* rule.

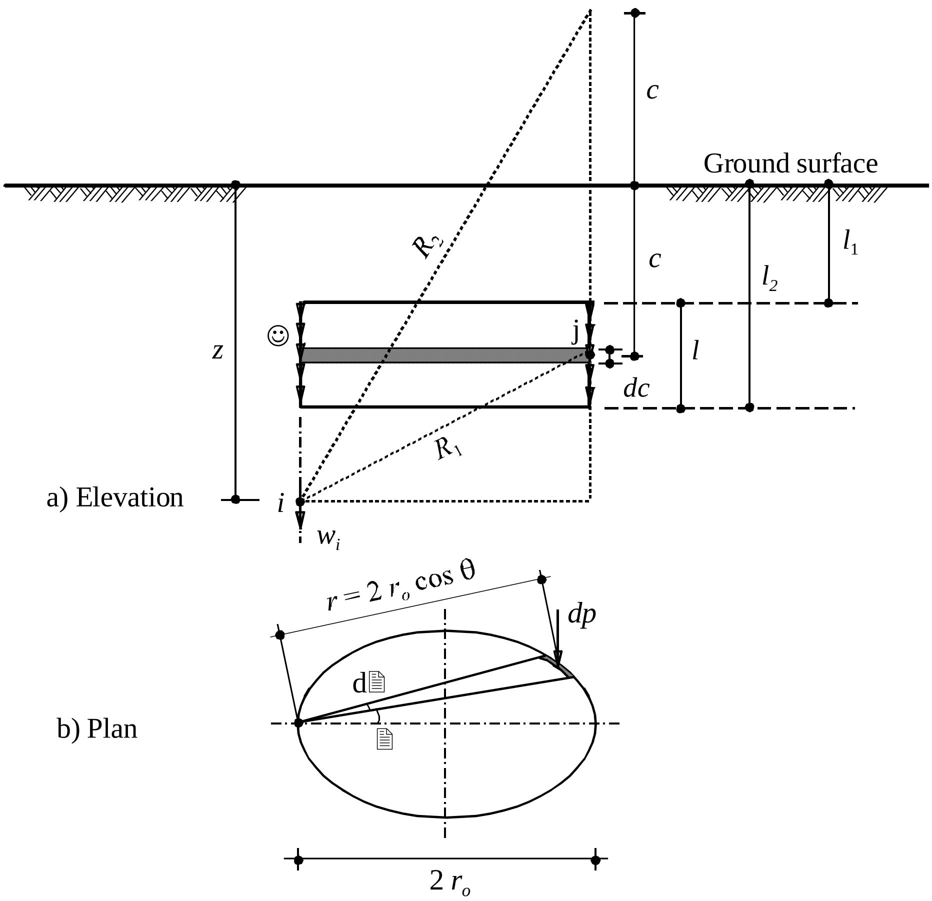

Figure 1.6 Geometry of cylindrical surface stress for finding the displacement at edge.

The factors are evaluated through numerical integration to determine the displacement factors for nodes located at the pile shaft. An equivalent line load replaces shaft stress to avoid the significant computations when applying *Mindlin's* solution to determine the displacement factors for nodes located outside the pile, while an equivalent point load replaces a circular load at the base.

1.3 Determining flexibility coefficients

The pioneer authors of the piled raft, such as *Poulos & Davis* (1968) [16] and *Butterfield & Banerjee* (1971) [4], integrated coefficients of flexibility numerically using *Mindlin's* solution (*Mindlin* (1936) [13]). Analysis of piled raft using numerical coefficients leads to significant computations, especially in large pile group problems. An analytical derivation of coefficients of flexibility using *Mindlin's* solution is presented.

1.3.1 Flexibility coefficient $f_{i,\,b}$ of a node *i* due to a unit force on the base *b*

An equivalent point load replaces a circular load to avoid significant computations when applying *Mindlin's* solution to determine the flexibility coefficients for nodes located outside the base. In this case, the flexibility coefficient can be obtained directly from *Mindlin's* solution for determining the displacement w_{ij} [m] at point *i* due to a point load Q_j [kN] acting at point *j* beneath the surface of a semi-infinite mass (Figure 1.1).

The flexibility coefficient $f_{i,\,b}$ [m/kN] of node *i* due to a unit force Q_b = 1 [kN] acting on the base *b* is equal to the displacement factor f_{ij} in Eq. (1.2). In this case, *r* is the radial distance between point *i* and the base point *b*. For the pile of the studied base *b, r* is equal to the radius of the base r_o.

1.3.2 Flexibility coefficient $f_{b,\,b}$ of the base *b* due to a unit force on the base itself

The base *b* of the pile has a circularly loaded area of radius r_o [m] and a uniform load $q = Q_b / \pi\, r_o^2$ [kN/m^2], as shown in Figure 1.2. The flexibility coefficient $f_{b,\,b}$ [m/kN] at the base center *b* due to a unit load Q_b = 1 [kN] at the base itself can be obtained from:

$$f_{b,b} = \frac{1}{\pi\, r_o^2} \int_0^{2\pi} \int_0^{r_o} f_{ij}\, r\, dr\, d\theta \tag{1.21}$$

The integration of the flexibility coefficient can be obtained analytically as:

$$\begin{aligned} f_{b,b} = \frac{1}{8\,\pi\, r_o^2\, G_s\,(1-\nu_s)} \Bigg(& (3-4\nu_s)\, r_o + \left[8\,(1-\nu_s)^2 - (3-4\nu_s)\right]\left[\sqrt{r_o^2 + 4\,c^2} - 2\,c\right] \\ & + \left[4\,c^2\,(3-4\nu_s) - 2\,c^2\right]\left[\frac{1}{2\,c} - \frac{1}{\sqrt{r_o^2 + 4\,c^2}}\right] + \left[1 - \frac{8\,c^4}{\left(r_o^2 + 4\,c^2\right)^{3/2}}\right]\Bigg) \end{aligned} \tag{1.22}$$

The flexibility coefficient $f_{b,\,b}$ may be multiplied by a factor $\pi/4$ to take the effect of base rigidity. This factor is the ratio of the surface displacement of a rigid circle on the surface of a half-space to the center displacement of a corresponding uniformly loaded circle.

1.3.3 Flexibility coefficient $f_{i,\,j}$ of node *i* due to a unit force on a node shaft *j*

An equivalent line load replaces the shaft stress to avoid the significant computations when applying *Mindlin's* solution to determine the flexibility coefficients due to shaft stress. The shaft element *j* of the pile has a length *l* [m] and a line load $T = Q_j / l$ [kN/m], as shown in Figure 1.4. The flexibility coefficient $f_{i,\,j}$ [m/kN] at the point *i* due to a unit load Q_j = 1 [kN] at a shaft element *j* can be obtained from:

$$f_{i,j} = \frac{1}{l} \int_{l_1}^{l_2} f_{ij}\, dc \tag{1.23}$$

The integration yields to:

$$f_{i,j} = \frac{1}{16\,\pi\,l\,G_s\,(1-\nu_s)}\left(I_1 + I_2 + I_3 + I_4 + I_5\right) \qquad (1.24)$$

where terms I_1 to I_5 are given in Eq. (1.14) to Eq. (1.18).

1.3.4 Flexibility coefficient $f_{b,j}$ of the base *b* due to a unit force on a node shaft *j*

The base *b* of the pile has a radius r_o [m], while the shaft element *j* has a length *l* [m] and a shear stress $\tau = Q_j \,/\, 2\,\pi\, r_o\, l$ [kN/m^2], as shown in Figure 1.5. The flexibility coefficient $f_{b,j}$ [m/kN] at the base center *b* due to a unit load Q_j = 1 [kN] at a shaft element *j* can be obtained from:

$$f_{b,j} = \frac{1}{2\,\pi\,l}\int_0^{2\pi}\int_{l_1}^{l_2} f_{ij}\, dc\, d\theta \qquad (1.25)$$

The integration yields to:

$$f_{b,j} = \frac{1}{16\,\pi\,l\,G_s\,(1-\nu_s)}\left(J_1 + J_2 + J_3 + J_4 + J_5\right) \qquad (1.26)$$

Replacing r_1 by r_o in Eq. (1.14) to Eq. (1.18) gives terms J_1 to J_5.

1.3.5 Multi-layered soil

Flexibility coefficients described previously can be applied only for isotropic elastic half-space soil medium. For finite layers, flexibility coefficients may be obtained as described by *Poulos* & *Davis* (1968) [16]. As an example, for a point *k* in a layer of depth *h*, the flexibility coefficient is then:

$$f_{k,j}(h) = f_{k,j}(\infty) - f_{h,j}(\infty) \qquad (1.27)$$

where:

$f_{k,j}(h)$ Flexibility coefficient for a point *k* in a layer of depth *h* due to a unit load on point *j*, [m/kN].

$f_{k,j}(\infty)$ Flexibility coefficient for a point *k* due to a unit load on point *j*, in a semi-infinite mass, [m/kN].

$f_{h,j}(\infty)$ Flexibility coefficient for a point within the semi-infinite mass directly beneath *k*, at a depth *h* below the surface due to a unit load on point *j*, [m/kN].

1.4 Modeling single pile

In standard methods of analyzing piled rafts based on elasticity theory, the entire soil stiffness matrix of the piled raft is assembled due to all elements of piles and raft. Then, settlements of piled raft elements are obtained directly by solving the global equations. Based on elasticity theory *El Gendy* (2007) [7] presented a more efficient analysis of single pile, pile group, and piled raft by using the composed coefficient technique to reduce the size of the entire soil stiffness matrix. In this technique, the pile is treated as a rigid member having a uniform settlement on its nodes. This assumption enables assembly pile coefficients in composed coefficients. It can easily model the nonlinear response of single pile, pile groups, or piled rafts. The composed coefficient technique makes the soil stiffness matrix of the piled raft size equivalent to that of the raft alone without piles. The proposed analysis considerably reduces the number of equations that need to be solved. The raft can be analyzed as flexible, rigid, or elastic on a continuum soil medium. The advantage of the analysis is that there is no approximation when generating the flexibility coefficients of the soil. In this analysis, the full interaction among piled raft elements is taken into account by generating the entire flexibility matrix of the piled raft. Using the composed coefficient technique enables the application of the nonlinear response of the pile by a hyperbolic relation between the load and settlement of the pile. Also, *El Gendy* (2007) [7] introduced a direct hyperbolic function for the nonlinear analysis of a single pile. Besides, an iteration method is developed to solve the nonlinear equations system of pile groups or piled rafts. This book presents numerical modeling single pile according to *El Gendy* (2007) [7].

To carry out the analysis, a composed coefficient or modulus *ks* [kN/m] representing the linear soil stiffness of the pile is determined. The modulus *ks* is a parameter used in both linear and nonlinear analysis of the pile. It is defined as the ratio between the applied force on the pile head *Ph* [kN] and the pile settlement *wo* [m]. The modulus *ks* is not a soil constant. It depends on pile load, pile geometry, and the stratification of the soil. It is analogous to the modulus of subgrade reaction of the raft on *Winkler's* soil medium (*Winkler* (1867) [20]), which is the ratio between the average contact pressure and the settlement under the characteristic point on the raft. This section describes a method to obtain the modulus *ks* from the rigid analysis of the pile.

1.4.1 Soil flexibility for single pile

In the analysis, the pile is divided into shaft elements with *m* nodes, each acted upon by a uniform shear stress qs_j [kN/m^2] and a circular base with a uniform stress *qb* [kN/m^2], as shown in Figure 1.7a. Pile shaft elements are represented by line elements to carry out the analysis, as indicated in Figure 1.7b. All stresses acting on shaft elements are replaced by a series of concentrated forces acting on line nodes. The shear force on node *j* may be expressed as:

$$Qs_j = 2\pi\, r_o \frac{l_{j-1} + l_j}{2} qs_j \tag{1.28}$$

while the force on the pile base may be expressed as:

$$Qb = \pi\, r_o^2 qb \tag{1.29}$$

where:

j - 1 and *j*	Node number of element *j*
Qs_j	Shear force on node *j* [kN]
Qb	Force on the base [kN]
r_o	Radius of the pile [m]
l_j	Length of the element *j* [m]

The soil is represented as a layered or isotropic elastic half-space medium to consider the interaction between pile and soil. Assuming a typical node i as shown in Figure 1.7b, the settlement s_i of the soil adjacent to the node i due to shear forces Qs_j on all m nodes and due to the base force Qb is expressed as:

$$s_i = \sum_{j=1}^{m} f_{i,j}\, Qs_j + f_{i,b}\, Qb \qquad (1.30)$$

where:

$f_{i,j}$ Flexibility coefficient of node i due to a unit shear force on a node shaft j [m/kN]

$f_{i,b}$ Flexibility coefficient of node i due to a unit force on the base b [m/kN]

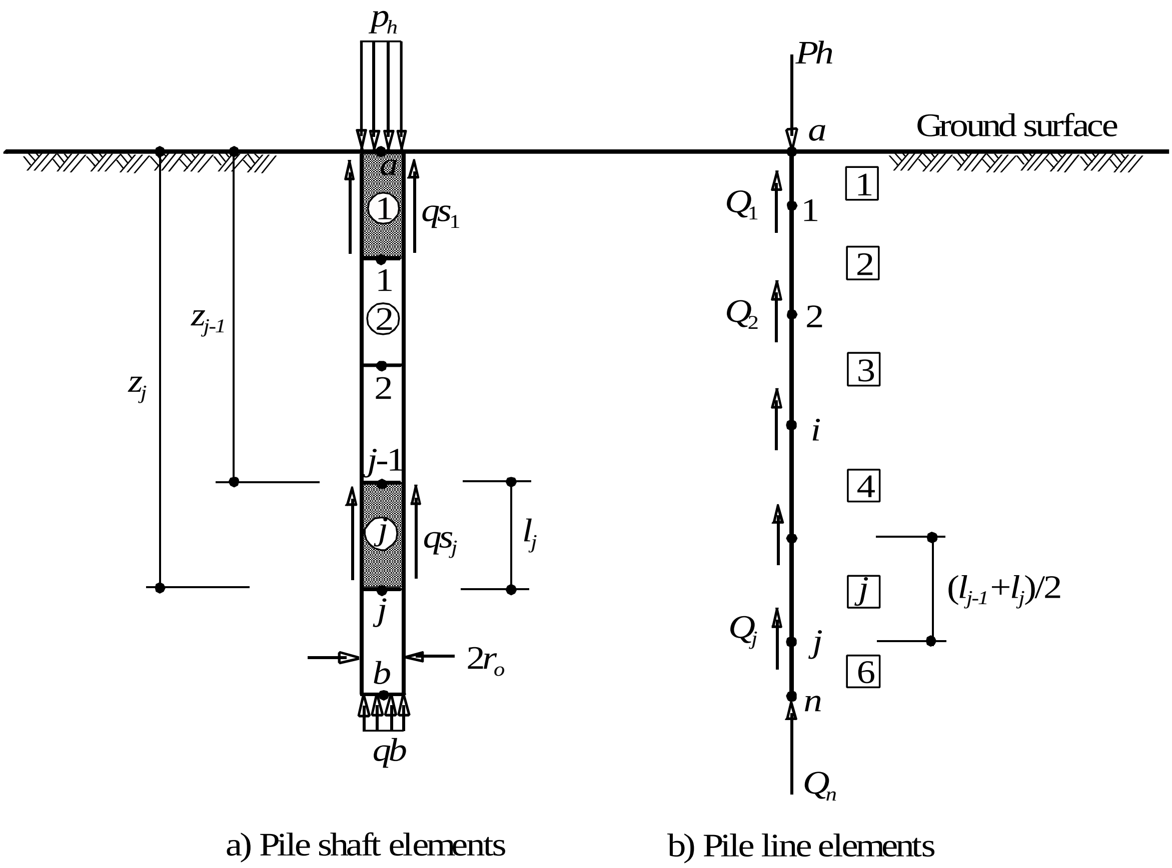

Figure 1.7 Pile geometry and elements.

As a special case of Eq. (1.30) and by changing the index i to b, the settlement of the base s_b may be expressed as:

$$s_b = \sum_{j=1}^{m} f_{b,j}\, Qs_j + f_{b,b}\, Qb \qquad (1.31)$$

where:

$f_{b,j}$ Flexibility coefficient of the base b due to a unit shear force on a node shaft j [m/kN]

$f_{b,b}$ Flexibility coefficient of the base b due to a unit force on the base b [m/kN]

Equations (1.30) and (1.31) for the settlement of the soil adjacent to all nodes of the pile may be rewritten in general form as:

$$w_i = \sum_{j=1}^{n} I_{i,j}\, Q_j \tag{1.32}$$

where:

Q_j Contact force on node j [kN]. Q_j represents the shear forces Qs_j on the shaft nodes or a base force Qb

w_i Settlement on node i [m]. w_i represents the settlement s_j on a shaft node j or settlement s_b on the base

n Total number of contact nodes, $n = m + 1$

$I_{i,j}$ Flexibility coefficient of node i due to a unit force on node j [m/kN]. $I_{i,j}$ represents the coefficient $f_{i,j}$, $f_{i,b}$, $f_{b,j}$ or $f_{b,b}$. These coefficients can be evaluated from elastic theory using *Mindlin's* solution. Closed-form equations for these coefficients are described in the next paragraph

1.4.2 Elastic analysis of single pile

1.4.2.1 Soil settlement

Equation (1.32) for settlements of the soil adjacent to all nodes of the pile may be written in a matrix form as:

$$\{w\} = [Is]\{Q\} \tag{1.33}$$

where:

$\{w\}$ n settlement vector

$\{Q\}$ n contact force vector

$[Is]$ n * n soil flexibility matrix

Inverting the soil flexibility matrix in Eq. (1.33), leads to:

$$\{Q\} = [ks]\{w\} \tag{1.34}$$

where $[ks]$ is n * n soil stiffness matrix, $[ks] = [Is]^{-1}$.

Equation (1.34) may be modified as:

$$\begin{Bmatrix} 0 \\ Qs_1 \\ Qs_2 \\ Qs_3 \\ \ldots \\ Qb \end{Bmatrix} = \begin{bmatrix} 0 & 0 & 0 & 0 & 0 & 0 \\ 0 & k_{1,1} & k_{1,2} & k_{1,3} & \ldots & k_{1,n} \\ 0 & k_{2,1} & k_{2,1} & k_{2,1} & \ldots & k_{2,n} \\ 0 & k_{3,1} & k_{3,1} & k_{3,1} & \ldots & k_{3,n} \\ 0 & \ldots & \ldots & \ldots & \ldots & \ldots \\ 0 & k_{n,1} & k_{n,1} & k_{n,1} & \ldots & k_{n,n} \end{bmatrix} \begin{Bmatrix} 0 \\ s_1 \\ s_2 \\ s_3 \\ \ldots \\ sb \end{Bmatrix} \tag{1.35}$$

Equation (1.35) is rewritten in a compacted matrix form as:

$$\{Qs\} = [ke]\{s\} \tag{1.36}$$

where:

$\{s\}$ $n + 1$ settlement vector, $\{s\} = \{o, s1, s2, s3, \ldots, sn, sb\}^T$

$\{Qs\}$ $n + 1$vector of contact forces on the pile, $\{Q\} = \{o, Qs1, Qs2, Qs3, \ldots, Qsn, Qb\}^T$

$[ke]$ $n + 1$ * $n + 1$ soil stiffness matrix

1.4.2.2 Pile displacement

The finite element method is used for analyzing the pile. Only the axial compression of the pile is considered in determining displacements of pile elements. The beam stiffness matrix of the pile element *i* can be expressed as:

$$[kp]_i = \frac{Ep \cdot Ap_i}{l_i}\begin{bmatrix} 1 & -1 \\ -1 & 1 \end{bmatrix} \quad (1.37)$$

where:

Ep Modulus of Elasticity of the pile material [kN/m^2]
Ap_i Cross-section area of the pile element *i* [m^2]
l_i Length of the pile element *i* [m]

According to the principal of the finite element method, the assembled axial stiffness matrix equation for the pile can be written as:

$$[kp]\{\delta\} = \{P\} - \{Qs\} \quad (1.38)$$

where:

$\{\delta\}$ n + 1 Displacement vector
$\{P\}$ n + 1 vector of applied load on the pile, $\{P\} = \{Ph, o, o, o, \ldots, o\}^T$
$[kp]$ $n + 1 * n + 1$ beam stiffness matrix

Substituting Eq. (1.36) in Eq (1.38) leads to:

$$[kp]\{\delta\} = \{P\} - [ke]\{s\} \quad (1.39)$$

Assuming full compatibility between pile displacement δ_i and soil settlement s_i, the following equation can be obtained:

$$[[kp] + [ke]]\{\delta\} = \{P\} \quad (1.40)$$

Solving the above system of linear equations gives the displacement at each node equal to the soil settlement at that node. Substituting soil settlements from Eq. (1.40) in Eq. (1.36) provides contact forces on the pile.

1.4.3 Rigid analysis of single pile

For a rigid pile, the settlement will be uniform. Therefore, the unknowns of the problem are *n* contact forces Q_j and the rigid body translation *wo*. The derivation of the uniform settlement for the rigid pile can be carried out by equating the settlement w_i in Eq. (1. 32) by a uniform translation *wo* at all nodes on the pile. Expanding Eq. (1. 32) for all nodes yields to:

$$\left.\begin{aligned}
w_1 &= wo = I_{1,1}Q_1 + I_{1,2}Q_1 + I_{1,3}Q_1 + ... + I_{1,n}Q_n \\
w_2 &= wo = I_{2,1}Q_1 + I_{2,2}Q_1 + I_{2,3}Q_1 + ... + I_{2,n}Q_n \\
w_3 &= wo = I_{3,1}Q_1 + I_{3,2}Q_1 + I_{3,3}Q_1 + ... + I_{3,n}Q_n \\
&... \\
w_n &= wo = I_{n,1}Q_1 + I_{n,2}Q_1 + I_{n,3}Q_1 + ... + I_{n,n}Q_n
\end{aligned}\right\} \tag{1.41}$$

Contact forces can be written as a function in terms $k_{i,j}$ of the soil stiffness matrix [ks] as:

$$\left.\begin{aligned}
Q_1 &= k_{1,1}wo + k_{1,2}wo + k_{1,3}wo + ... + k_{1,n}wo \\
Q_2 &= k_{2,1}wo + k_{2,2}wo + k_{2,3}wo + ... + k_{2,n}wo \\
Q_3 &= k_{3,1}wo + k_{3,2}wo + k_{3,3}wo + ... + k_{3,n}wo \\
&... \\
Q_n &= k_{n,1}wo + k_{n,2}wo + k_{n,3}wo + ... + k_{n,n}wo
\end{aligned}\right\} \tag{1.42}$$

Carrying out the summation of all contact forces leads to:

$$\sum_{i=1}^{n} Q_i = wo \sum_{i=1}^{n} \sum_{j=1}^{n} k_{i,j} \tag{1.43}$$

Equation (1.43) may be rewritten as:

$$Ph = ks\, wo \tag{1.44}$$

where the applied force Ph [kN] is the sum of all contact forces Q_i:

$$Ph = \sum_{i=1}^{n} Q_i \tag{1.45}$$

while the composed coefficient ks [kN/m] is the sum of all coefficients of the soil stiffness matrix [ks]:

$$ks = \sum_{i=1}^{n} \sum_{j=1}^{n} k_{i,j} \tag{1.46}$$

Eq. (1.44) gives the linear relation between the applied load on the pile head and the uniform settlement wo, analogous to *Hook's* law. Therefore, the composed coefficient ks may be used to determine the total soil stiffness adjacent to the pile. In analyzing a single pile, it is easy to determine the contact forces Q_i. Substituting the value of wo from Eq. (1.44) in Eq. (1.47) gives Eq. (1.42) in n unknown contact forces Q_i as:

$$Q_i = \frac{Ph \sum_{j=1}^{n} k_{i,j}}{ks} \tag{1.47}$$

Equation (1.47) of contact forces on the rigid pile is found to be independent of the Modulus of elasticity of the soil E_s in the case of isotropic elastic half-space soil medium.

1.4.4 Nonlinear rigid analysis of single pile

Nonlinear analysis is an important consideration since piles may be loaded close to their maximum capacity, even under working conditions. A hyperbolic relation between the pile load and settlement is considered to determine the nonlinearity of the pile. Figure 1.8 shows a typical nonlinear curve of load-settlement for a wide range of soils. The curve is approximated through a hyperbolic interpolation formula where several equation forms are available to verify this curve.

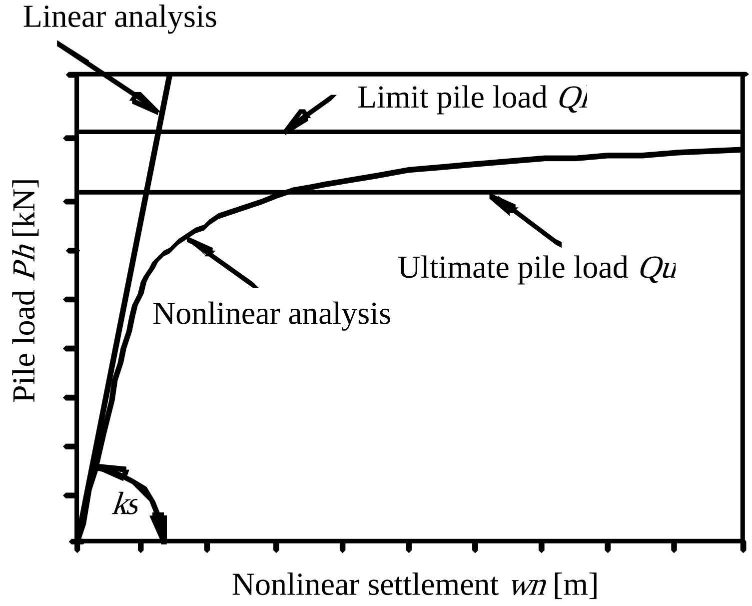

Figure 1.8 Load-settlement curve of a single pile (hyperbolic relation).

Many methods were developed to study pile-soil systems with the nonlinear response using a hyperbolic relation between the load and settlement. *Yamashita* (1987) [21] present an analytical solution of a single pile and pile group based on *Mindlin's* solution and introduced an equation representing the hyperbolic relationship between load and displacement. Also, *Fleming* (1992) [9] developed a method to analyze and predict the load-deformation behavior of a single pile using two hyperbolic functions describing the shaft and base performance individually under applied load. Analyzing nonlinear behavior by hyperbolic function was used by *Mandolini/ Viggiani* (1997) [12] for pile groups and was used by *Russo* (1998) [17] for the piled raft. They considered piles as nonlinear interacting springs based on the method of interaction factors. *Basile* (1999) [1] assumed *Young's* modulus of the soil varies with the stress level at the pile-soil interface using a hyperbolic stress-strain relationship.

Available nonlinear analysis of foundation on *Winkler's* soil medium was presented by *Baz* (1987) [3] for the grid and by *Hasnien* (1993) [10] for the raft. *El Gendy* (1999) [6] extended this analysis to be applicable for a raft on a continuum soil medium. The composed coefficient technique described in the previous sections enables to apply this analysis on pile problems.

The nonlinear behavior of the pile head force-settlement at the piled raft-soil interface may be represented as:

$$Ph = \frac{wn}{\frac{1}{ks} + \frac{wn}{Ql}} \tag{1.48}$$

where:

wn Nonlinear settlement of the pile [m]
Ql Limit pile load [kN]

In Figure 1.8 and Eq. (1.48), the initial tangent modulus for a single pile is easily obtained from linear analysis of the pile. This modulus is equal to the modulus of soil stiffness *ks*. The limit pile load *Ql* is a geometrical parameter of the hyperbolic relation. In some cases, the value of *Ql* is different from the actual ultimate pile load. For a single pile, the force on the pile head *Ph* is known. Therefore, Eq. (1.48) gives the nonlinear settlement of the pile *wn* directly.

1.5 Defining the project data

1.5.1 Firm Header

When printing the results, the main data (firm name) are displayed on each page at the top in two lines or in a graphic presentation at the identification box. Firm name can be defined, modified, and saved using the "Firm Header" Option from the setting Tab (see Figure 1.9).

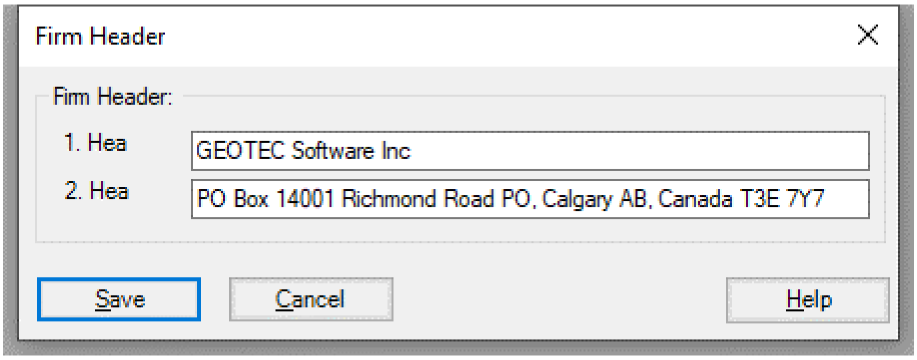

Figure 1.9 Firm Header.

1.5.2 Task of the program *GEO Tools* (Analysis Type)

GEO Tools program can be used to analyze various problems in Geotechnical Engineering for deep foundations and deep foundations, Figure 1.10.

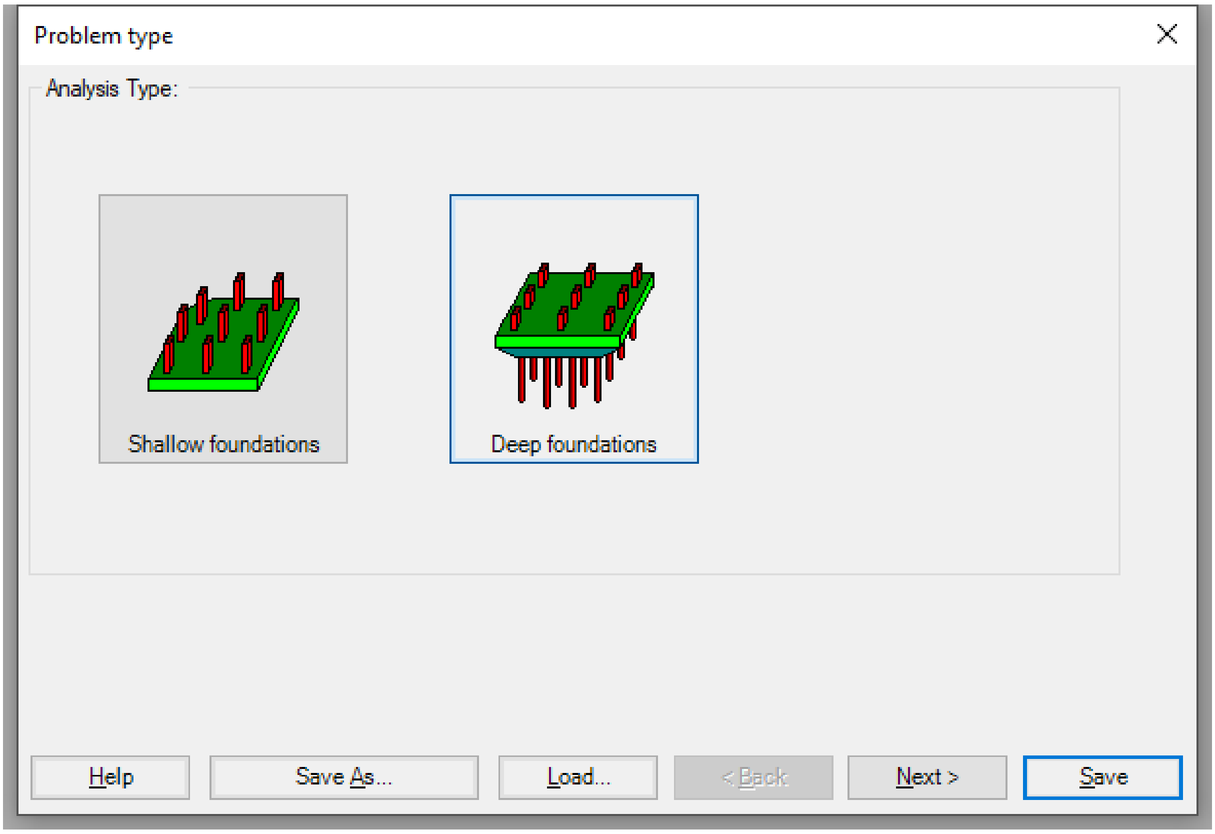

Figure 1.10 Problem type.

According to the main menu shown in Figure 1.10, the following geotechnical problems can be analyzed for shallow foundations:

1. Analysis of single pile
2. Bearing capacity and settlement of single pile or pile wall
3. Analysis of piled raft
4. Stress coefficients according to GEDDES
5. Sheet pile wall
6. Analysis of single barrette
7. Analysis of barrette raft

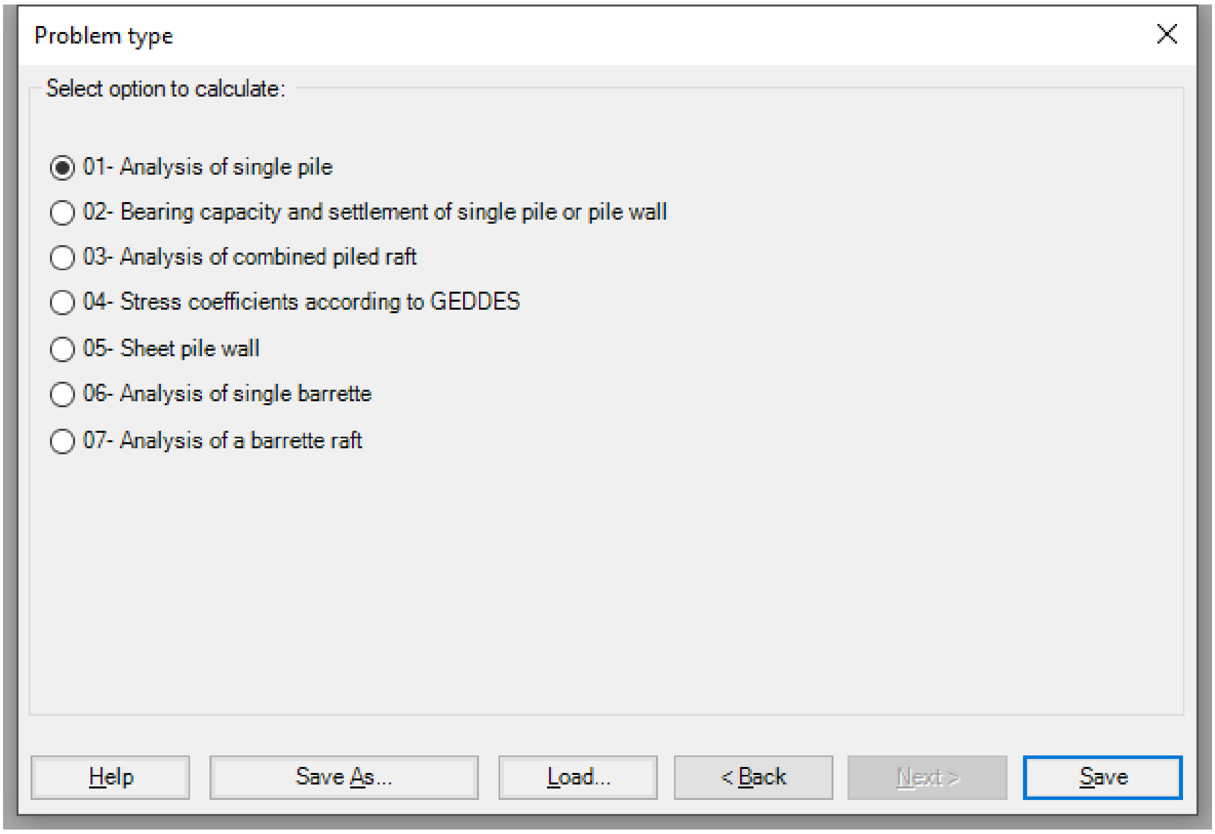

Figure 1.11 Problem type for deep foundation.

In menu of Figure 1.10 select the option:

01- Analysis of single pile

The following paragraph describes how to analyze a problem of the single pile by the program *GEO Tools*. The input data are the dimensions of the pile, pile load, pile material, and the properties of the soil layers.

1.5.3 Project Identification

In the program, it must be distinguished between the following two data groups:

1 System data (For identification of the project that is created and information to the output for the printer).

2 Soil data (Soil properties and so on).

The defining input data for these data groups is carried out as follows:

After clicking on the "Project Identification" option, the following general project data are defined (Figure 1.12):

Title: Title label
Date: Date
Project: Project label

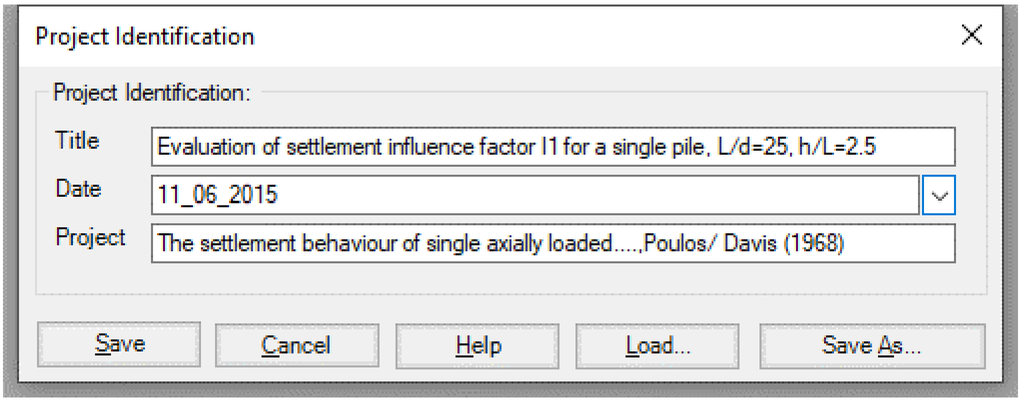

Figure 1.12 Project Identification.

1.5.4 Defining the single pile data

After clicking on the "Analysis of single pile" option, the following data of the pile problem are defined (Figure 1.13):

Pile material:

- *Gp* unit weight of pile concrete [kN/m^3]
- *Ep* Modulus of elasticity of pile [kN/m^2]

Pile data:

- *D* Pile diameter [m]
- *Lg* Pile length [m]
- *Ph* Load on pile head [kN]
- *Ql* Limit pile load [kN]
- *H* Lateral load on pile [kN]
- *M* Bending moment on pile [kN.m]
- *Hli* Lateral limit pile load [kN]

Calculation Task:

- Linear Analysis
- Nonlinear Analysis

Subsoil model:

- Half space-model
- Layered soil model

Element:

- *Dz* Depth increment in *z*-direction [m]

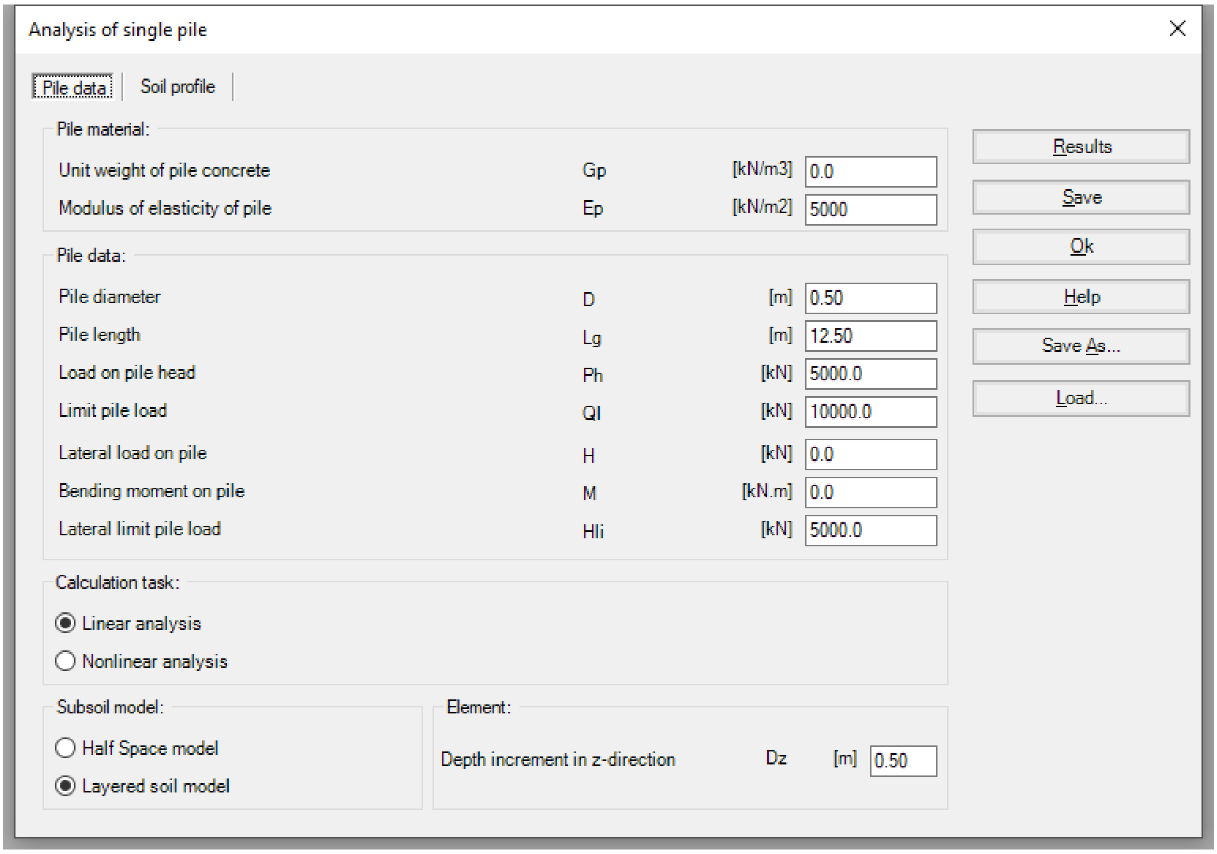

Figure 1.13 Analysis of single pile.

1.5.5 Data of soil layers

After clicking on "Soil profile" option in the form of Figure 1.13, the following properties of the soil layers are required to define (Figure 1.14):

-	Level of layer underground	*Z*	[m]
-	Modulus of elasticity of soil	*Es*	[kN/m^2]
-	Poisson's ratio of soil	*Nue*	[-]

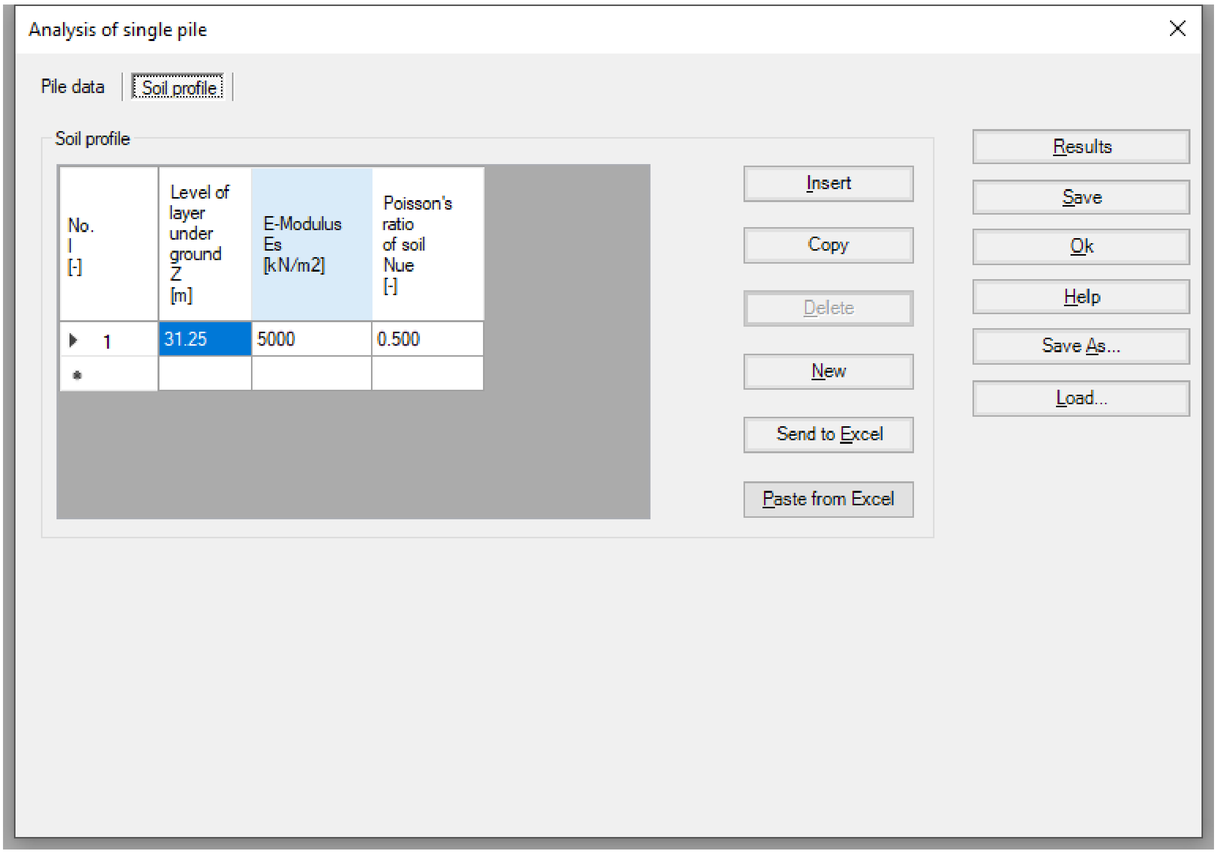

Figure 1.14 Soil data

1.6 Examples to verify single pile analysis

A user-friendly computer program, *GEO Tools* [8], has been developed for analyzing the single pile using different subsoil models. With the help of this program, an analysis of various examples was carried out to verify and test the methods and the program for analyzing single pile problems.

1.6.1 Example 1: Evaluation of settlement influence factor for a single pile

1.6.1.1 Description of the problem

Most piled raft analyses apply a numerical integration using *Mindlin's* solution to determine flexibility coefficients of piles. Applying a numerical integration in the piled raft analysis leads to significant computations, especially in large piled raft problems. In this case study, closed-form equations derived from *Mindlin's* solution are used in all calculations. The settlement influence factors *I1* for a single pile obtained by *Poulos* (1968) [14] and *Poulos/ Davis* (1968) [16] are compared with those obtained by closed-form equations listed in this book to verify these equations for determining flexibility coefficients.

From the analysis of a single pile carried out by *Poulos/ Davis* (1968), the settlement s_1 [m] of a single pile is expressed as:

$$s_1 = \frac{P}{L\,E_s} I_1 \tag{1.49}$$

where:

P Load on the pile head [kN]

L Pile length [m]

E_s *Young's* modulus of the surrounding soil mass [kN/m^2]

I_1 Settlement influence factor for a single pile [-]

A pile of length L = 12.5 [m] is chosen. The pile is divided into ten elements, each 1.25 [m]. Load on the pile head P and *Young's* modulus of the surrounding soil mass E_s are chosen to make the term P/E_s of Eq. (1.49) equal to unit. Thus, load on the pile head is P = 5000 [kN], while *Young's* modulus of the surrounding soil mass is E_s = 5000 [kN/m^2]. The settlement influence factor I_1 is determined at different values of h/L and L/d, where h [m] is the thickness of the soil layer and d [m] is the pile diameter.

1.6.1.2 Analysis and results

The settlement influence factors I_1 of a single pile published by *Poulos* (1968) [14] in Table 1 and Table 2 are compared with those obtained from the closed-form equations. The factors are tabulated for two different values of *Poisson's* ratio of the soil ν_s. From these tables, it can be observed that the settlement influence factors obtained by closed-form equations at different soil layers and pile diameters are nearly equal to those obtained by *Poulos* (1968) [14] with a maximum difference of Δ = 2.78 [%].

Table 1 Settlement influence factors I_1 [-] for a single pile
Using closed-form equations, *Poisson's* ratio of the soil $\nu_s = 0.5$ [-]

h/L	*Poulos* (1968) [14]			*ELPLA* [8]			Max. Diff. Δ [%]
	L/d			*L/d*			
	10	25	100	10	25	100	
∞	1.41	1.86	2.54	1.44	1.88	2.56	2.13
5	1.31	1.76	2.44	1.34	1.77	2.47	1.23
2.5	1.20	1.64	2.31	1.22	1.65	2.33	1.67
1.5	0.98	1.42	2.11	0.99	1.43	2.12	1.02
1.2	0.72	1.18	1.89	0.74	1.19	1.90	2.78

Table 2 Settlement influence factors I_1 [-] for a single pile
Using closed-form equations, *Poisson's* ratio of the soil $\nu_s = 0.0$ [-]

h/L	*Poulos* (1968) [14]			*ELPLA* [8]			Max. Diff. Δ [%]
	L/d			*L/d*			
	10	25	100	10	25	100	
∞	1.16	1.47	1.95	1.17	1.48	1.94	0.86
5	1.07	1.37	1.86	1.08	1.38	1.86	0.93
2.5	0.96	1.27	1.75	0.98	1.28	1.74	2.08
1.5	0.80	1.11	1.58	0.81	1.12	1.59	1.25
1.2	0.62	0.94	1.44	0.62	0.94	1.42	1.39

1.6.2 Example 2: Settlement of single compressible pile

1.6.2.1 Description of the problem

To verify the present analysis of a single pile within multi-layered soil, the settlement influence factors *I1* published by *Small/ Lee* (1992) [19], *De Sanctis* / *Russo* (2002) [5], and *Seo*/ *Prezzi* (2007) [18] are compared with those obtained by the present analysis of a single pile using flexibility coefficient.

An analytical analysis of a single pile embedded in a multi-layered soil medium is available in the reference *Small/ Lee* (1992) [19], *De Sanctis* / *Russo* (2002) [5], and *Seo*/ *Prezzi* (2007) [18]. *Small/ Lee* (1992) [19] and *Seo*/ *Prezzi* (2007) [18] compared results using the finite layer approach with those obtained by *Poulos* (1979) [15] using boundary element, boundary element equivalent modulus, and Finite Element and those obtained by *Lee* (1991) [11] using discrete layer. *De Sanctis* / *Russo* (2002) [5] compared results using the Boundary Element Method (BEM) based on the Steinbrenner approximation with those using the Finite Element.

The pile shown in Figure 1.15 is considered and analyzed for five different cases under different subsoil conditions. For all cases L/d = 25, h/L = 2, E_p/E_s = 1000, and *Poisson's* ratio ν_s = 0.3. The subsoil of each case consists of three layers except the last case, which has homogeneous soil. Each layer has a different Modulus of Elasticity E_s.

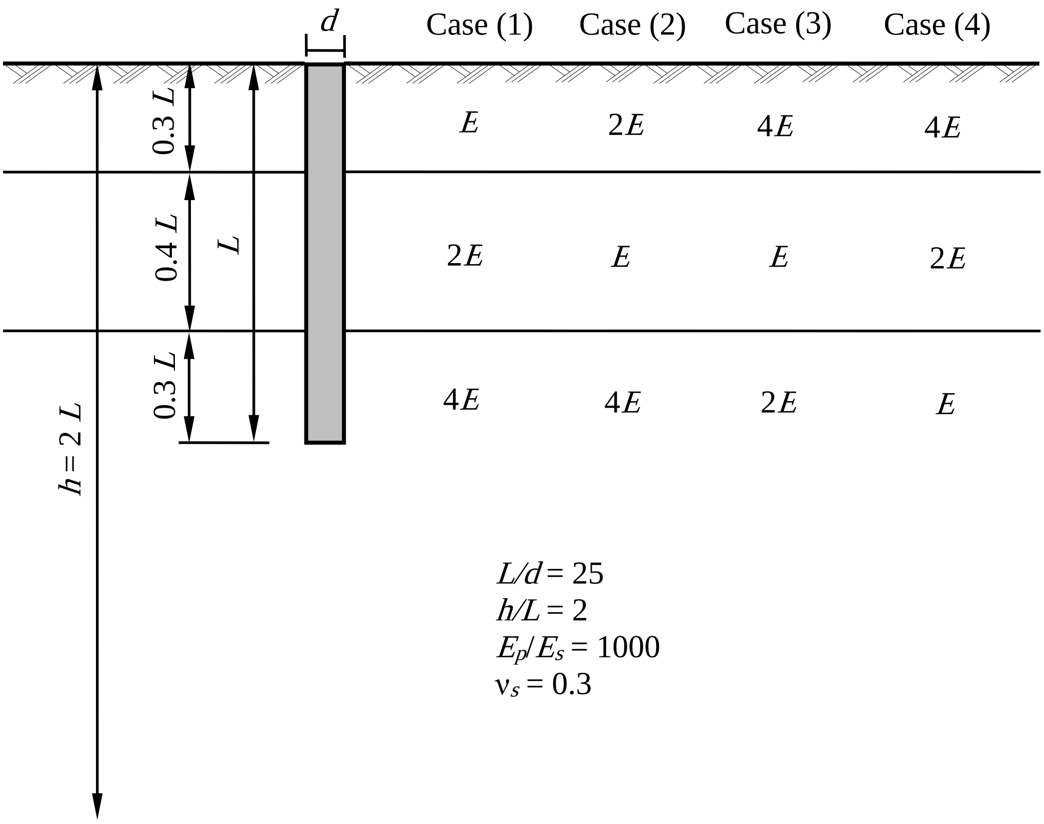

Figure 1.15 Single pile with subsoil, *De Sanctis* / *Russo* (2002) [5].

1.6.2.2 Analysis and results

The settlement influence factors I_1 of a single pile published by *Small/ Lee* (1992) [19], *De Sanctis* / *Russo* (2002) [5], and *Seo*/ *Prezzi* (2007) [18] in Table 3 are compared with those obtained from the closed-form equations. It can be observed that the settlement influence factors obtained by closed-form equations for different subsoil profiles are nearly equal to those of the references.

Table 3 Settlement influence factors I_1 [-] for a single pile

Cases		Case (1)	Case (2)	Case (3)	Case (4)	Homogeneous
Small/ Lee (1992) [19]	Boundary Element (*Poulos*, 1979) [15]	0.965	0.915	-	0.825	-
	Boundary Element Equivalent Modulus (*Poulos*, 1979) [15]	0.953	0.978	-	1.765	-
	Finite Element (*Poulos*, 1979) [15]	0.943	0.955	-	1.075	-
	Discrete Layer (*Lee*, 1991) [11]	0.903	0.895	-	0.930	-
	Finite Layer	0.915	0.933	-	1.035	-
De Sanctis / Russo (2002) [5]	Finite Element (ABAQUS)	0.862	0.876	0.929	1.027	1.731
	Boundary Element (Steinbrenner)	0.761	0.777	1.071	1.579	1.780
Seo/ Prezzi (2007) [18]	Analytical solutions	0.84	0.808	-	0.773	-
GEO Tools [8]	Closed-form equations	0.708	0.724	1.042	1.644	1.758 (Rigid) 2.059 (Elastic)

1.6.3 Example 3: Linear Analysis of Single pile

1.6.3.1 Description of the problem

The pile settlements with pile length obtained by the present linear analysis using flexibility coefficient are compared with those obtained by *Basu et al.* (2008) [2] to verify the presented analysis of a single pile in multi-layered soil. *Basu et al.* (2008) [2] developed an analytical solution of a single pile embedded in a multi-layered soil medium. Two cases are considered and analyzed, as shown in Figure 1.16 and Figure 1.17.

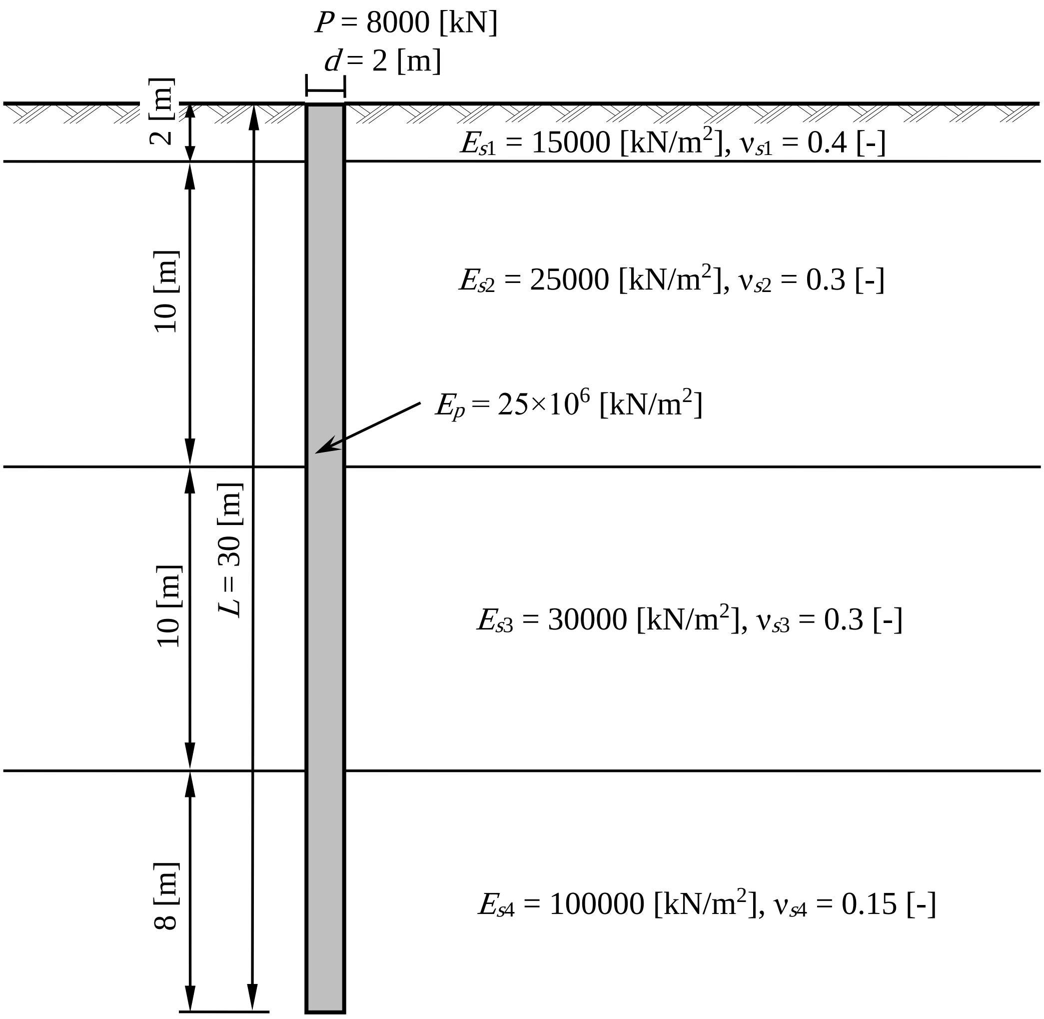

Figure 1.16 Single pile with subsoil, *Basu et al.* (2008) [2], Case (1).

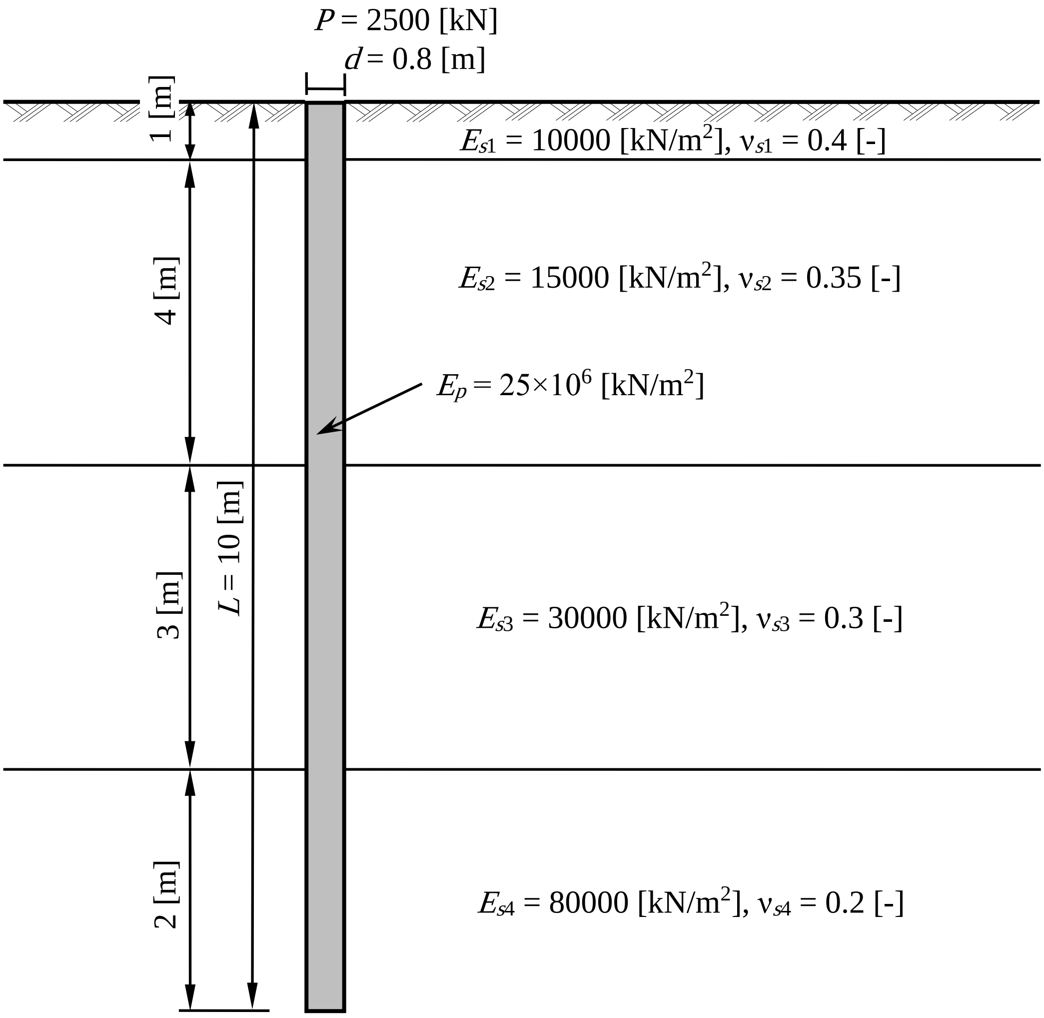

Figure 1.17 Single pile with subsoil, *Basu et al.* (2008) [2], Case (2).

1.6.3.2 Results

The pile settlement *s* along the pile length obtained from the present analysis using *GEO Tools* [8] are compared with *Basu et al.'s* (2008) [2] results, as shown in Figure 1.18 and Figure 1.19. These results indicate that the verification results of the present analysis are in good agreement with those of *Basu et al.* (2008) [2].

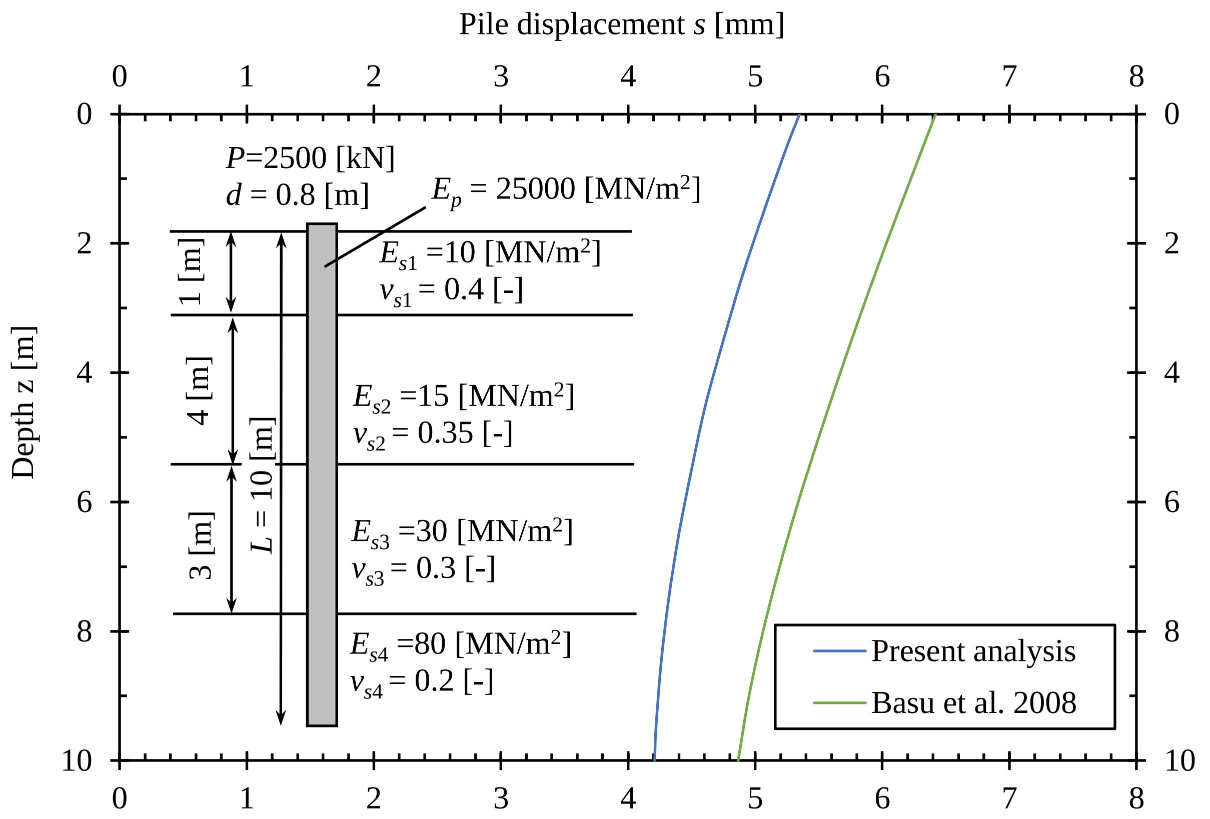

Figure 1.18 Settlement *s* [cm] along the pile length, Case (1).

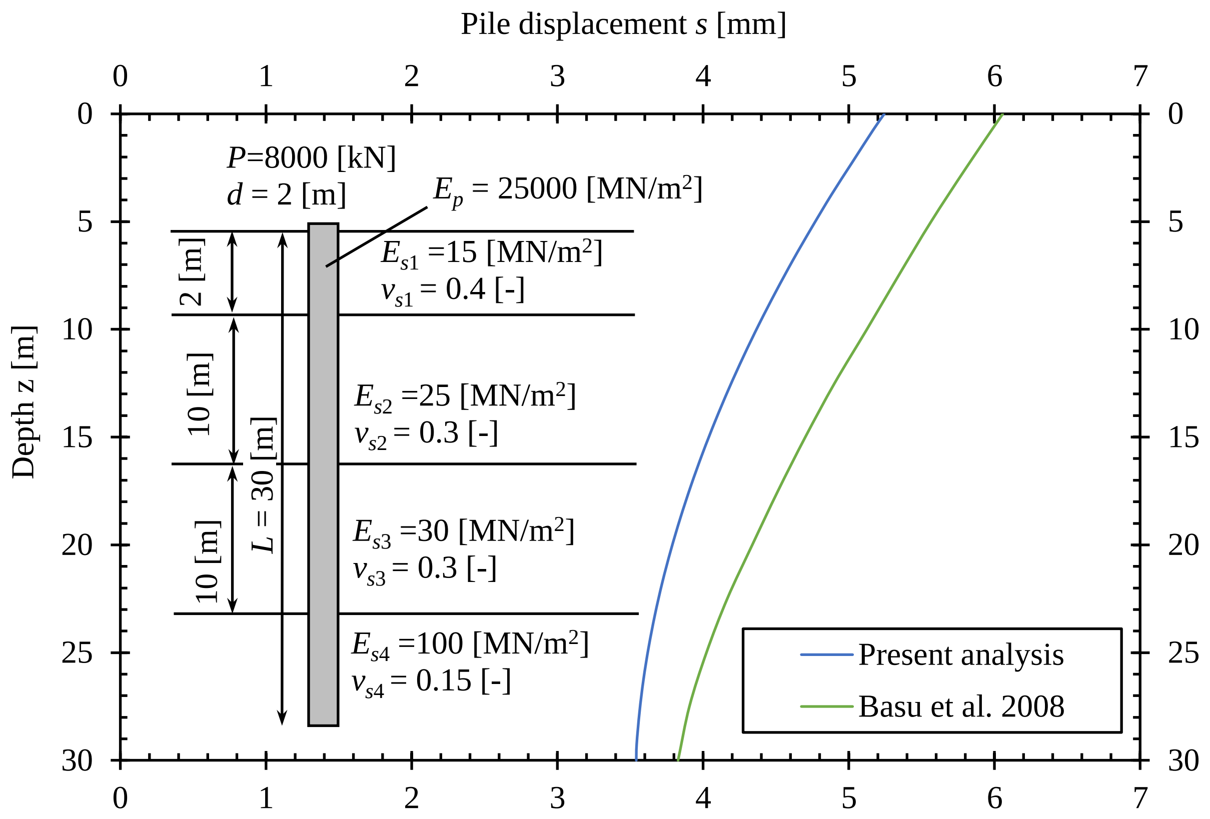

Figure 1.19 Settlement *s* [cm] along the pile length, Case (2).

1.6.4 Example 4: Nonlinear Analysis of Single pile

1.6.4.1 Description of the problem

The single pile results obtained by the present nonlinear analysis are compared with those obtained by *Seo*/ *Prezzi* (2007) [18] to verify the present nonlinear analysis of a vertically loaded single pile. *Seo*/ *Prezzi* (2007) [18] presented an analytical solution of a single pile embedded in a multi-layered soil medium and compared the results with a pile load test.

The single barrette shown in Figure 1.20 is analyzed nonlinearly with different vertical loads values. The subsoil of this case consists of three different layers. Each layer has a different modulus of elasticity E_s and *Poisson's* ratio ν_s.

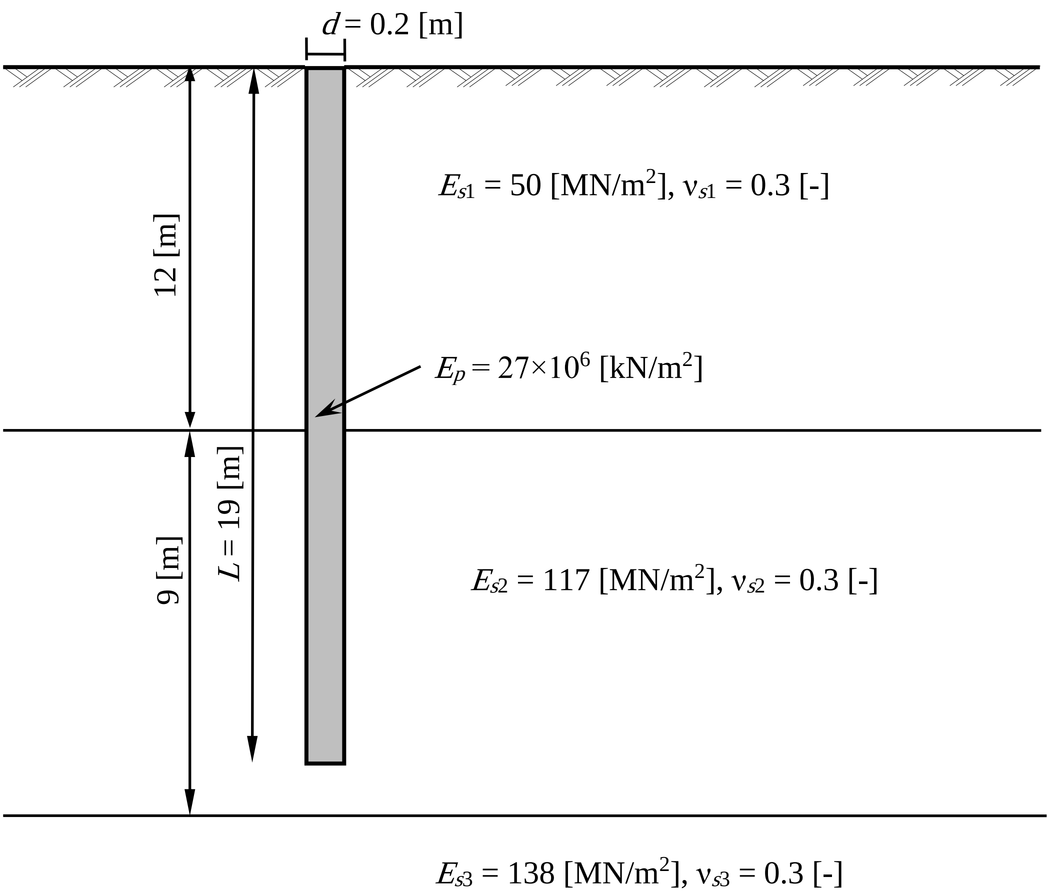

Figure 1.20 Single pile with subsoil, *Seo*/ *Prezzi* (2007) [18].

1.6.4.2 Results

The pile settlement *s* along the pile length obtained from the present analysis using *GEO Tools* [8] are compared with *Seo*/ *Prezzi's* (2007) [18] results, as shown in Figure 1.21 and Figure 1.22. These results indicate that the verification results of the present analysis are in good agreement with those of *Seo*/ *Prezzi* (2007) [18].

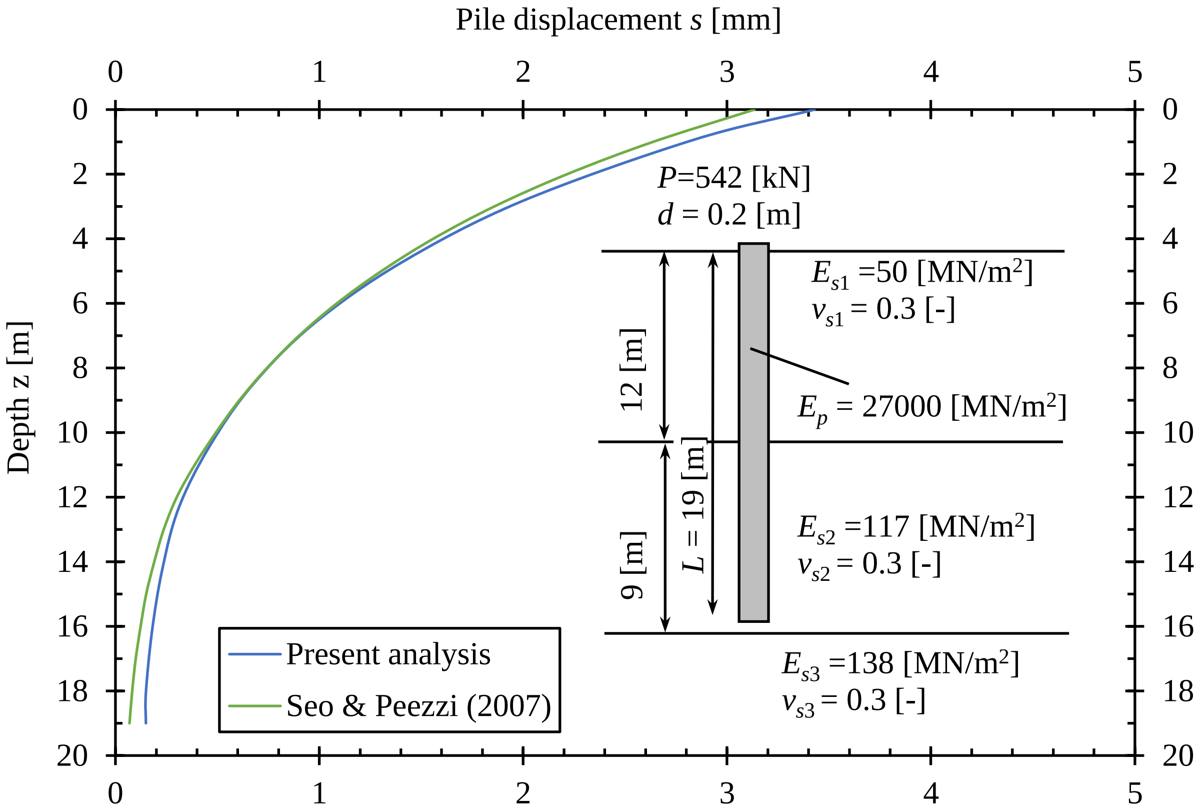

Figure 1.21 Settlement s [cm] along the pile length, P = 542 [kN].

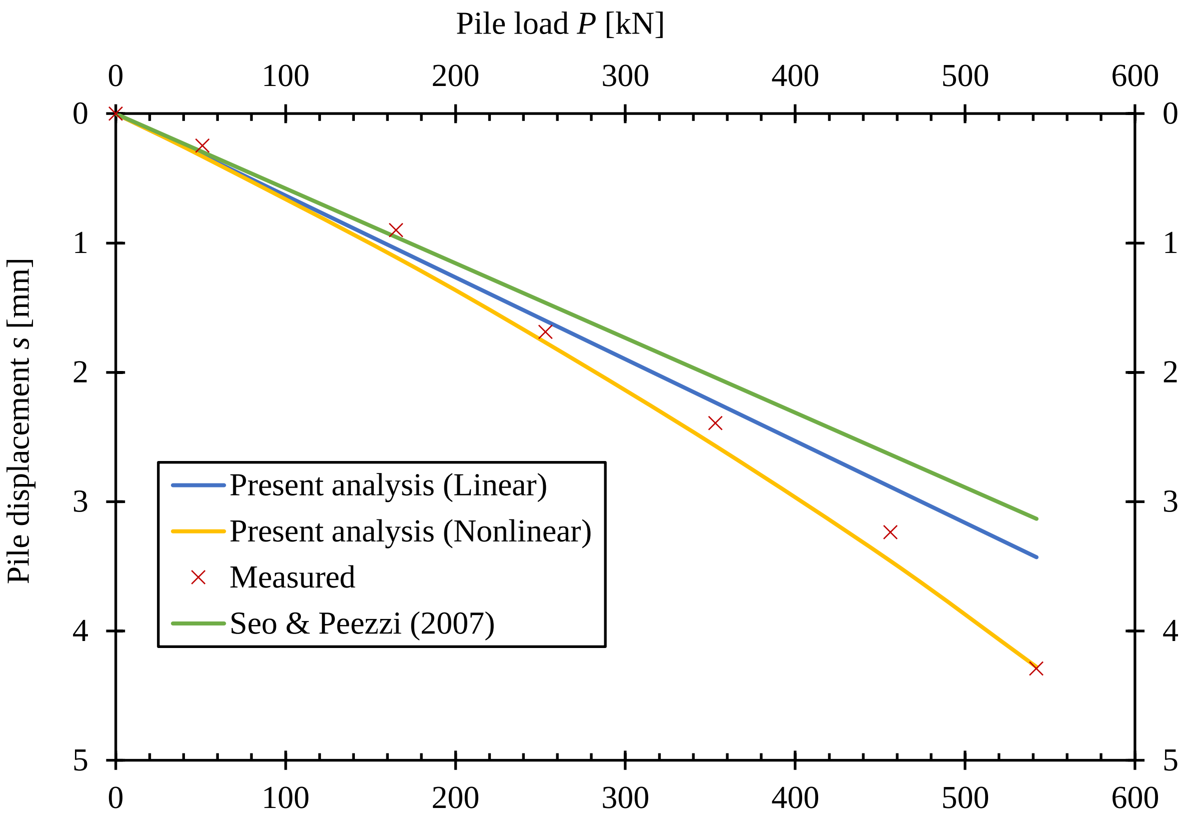

Figure 1.22 Load-displacement curve.

1.6.5 Example 5: Case Study of Load Tests

1.6.5.1 Description of the problem

To verify the present nonlinear analysis of a single pile in multi-layered soil, load-displacements obtained by the presented nonlinear analysis using *GEO Tools* [8] are compared with those measured results from pile load tests presented by *Yamashita et al.* (1987) [21]. For cases are considered and analyzed. Piles dimensions are listed in Table 4. The soil properties of each case are listed in Table 5.

Table 4 Piles dimensions

Case No.	1	2	3	4
Pile diameter d [m]	1.5	1.2	0.8	1.0
Pile length L [m]	46.6	16	44.4	34.4
Modulus of elasticity of the pile material E_p [MN/m^2]	2.75×10^6	2.6×10^6	2.6×10^6	3.0×10^6

Table 5 Soil properties

Case	Layer No. I	Layer depth from the ground surface z [m]	Modulus of elasticity E_s [MN/m^2]	*Poisson's* ratio ν_s [-]
1	1	4.6	42000	0.4
	2	9.2	63000	
	3	13.8	54900	
	4	18.4	66900	
	5	23	111600	
	6	27.6	153000	
	7	32.2	177000	
	8	36.8	198000	
	9	41.4	219000	
	10	46	243000	
	11	60	264000	
2	1	1.60	33000	0.3
	2	3.20	28800	
	3	4.80	36600	
	4	6.40	44400	
	5	8.00	46800	
	6	9.60	39000	
	7	11.20	34800	
	8	12.80	37200	
	9	14.40	43200	
	10	16.00	42000	
	11	30.00	44000	

Case	Layer No. I	Layer depth from the ground surface *z* [m]	Modulus of elasticity E_s [MN/m^2]	*Poisson's* ratio ν_s [-]
3	1	4.44	54000	0.4
	2	8.88	63000	
	3	13.32	84000	
	4	17.76	105000	
	5	22.20	126000	
	6	26.64	147000	
	7	31.08	168000	
	8	35.52	189000	
	9	39.96	234000	
	10	44.40	210000	
	11	60.00	249000	
4	1	3.43	0	0.3
	2	6.86	0	
	3	10.29	72000	
	4	13.72	87000	
	5	17.15	105000	
	6	20.58	106950	
	7	24.01	29400	
	8	27.44	36600	
	9	30.87	58200	
	10	34.30	69600	
	11	60.00	128000	

1.6.5.2 Results

The load-displacements obtained from the present analysis using *GEO Tools* [8] are compared with the pile load tests published in *Yamashita et al.* (1987) [21], as shown in Figure 1.23 to Figure 1.26. These results indicate that the verification results of the present analysis are in good agreement with those of *Yamashita et al.* (1987) [21].

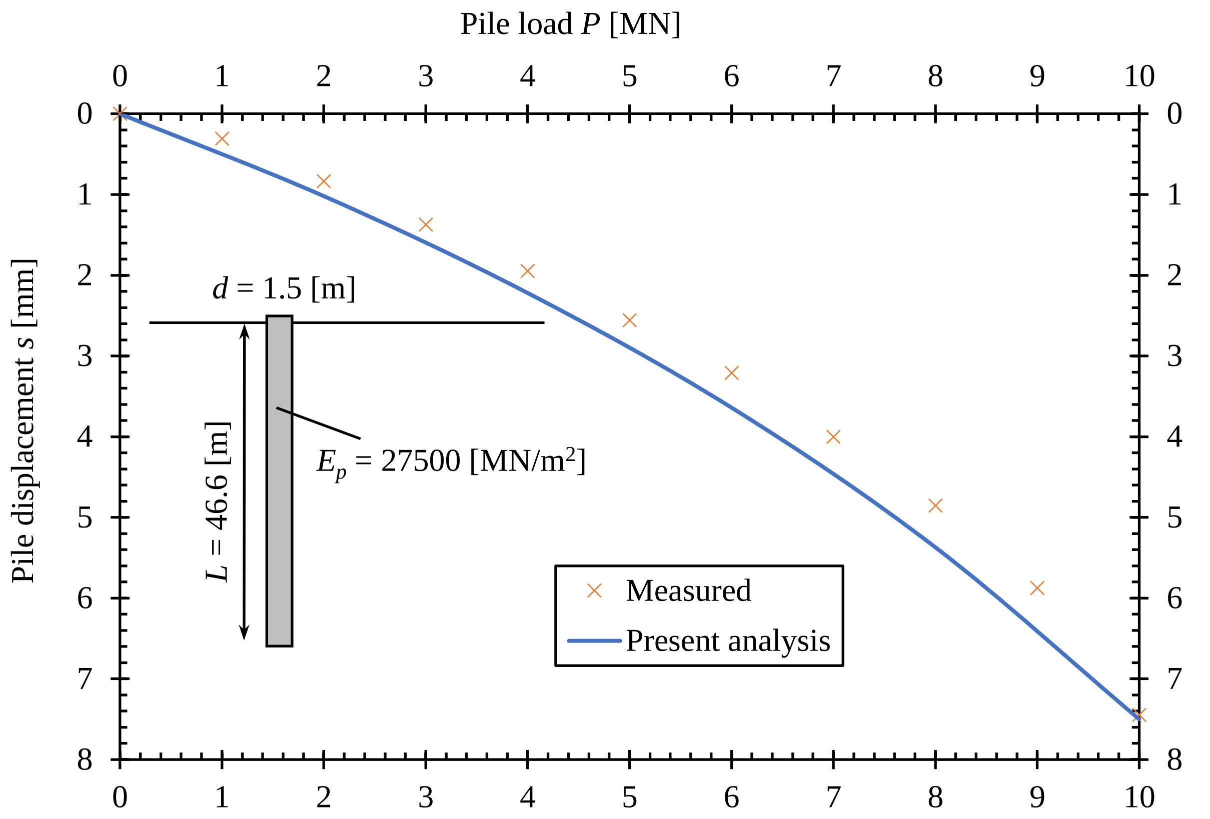

Figure 1.23 Load settlement curve, Case (1).

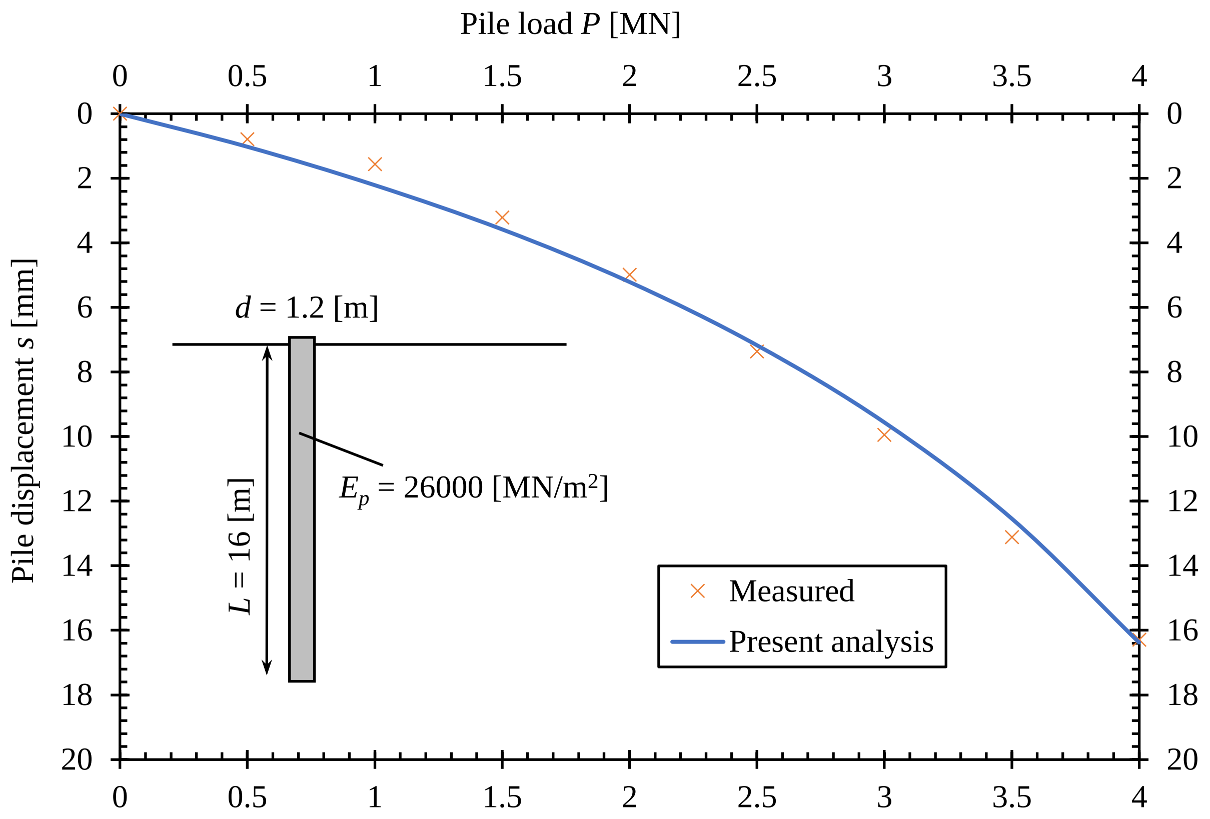

Figure 1.24 Load settlement curve, Case (2).

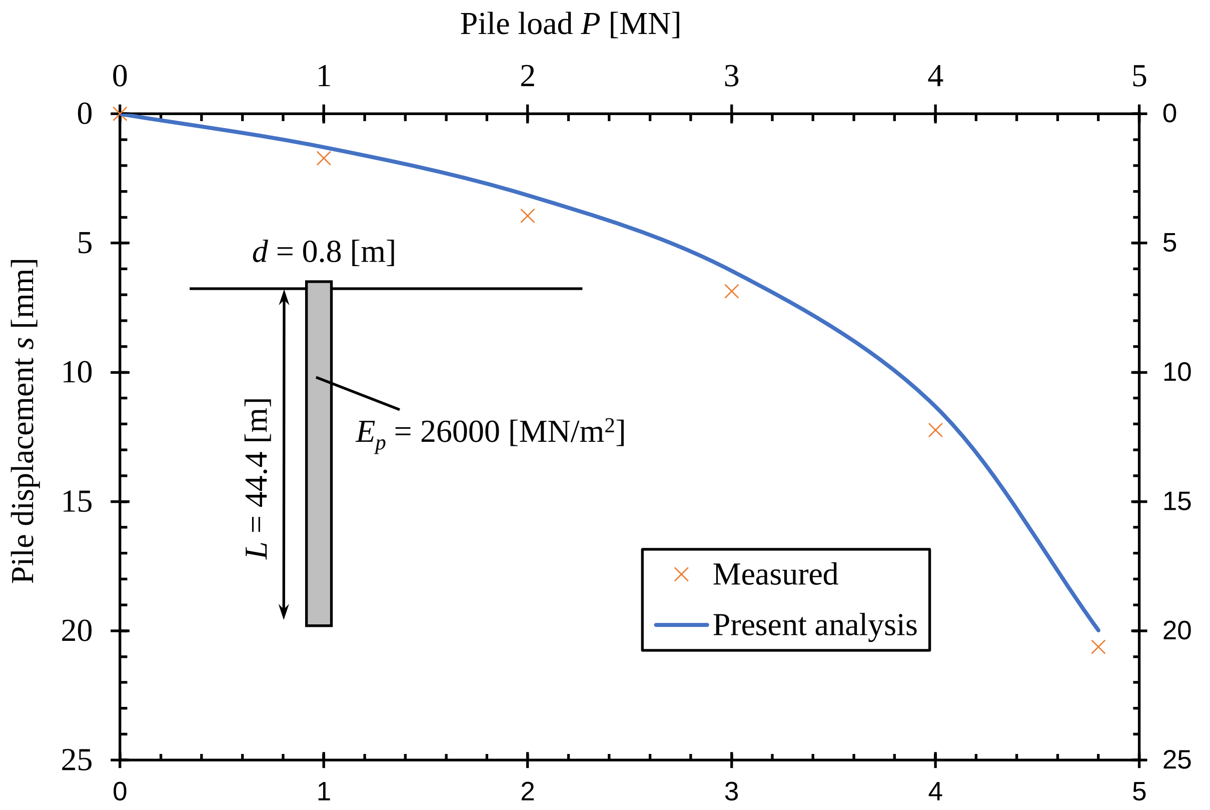

Figure 1.25 Load settlement curve, Case (3).

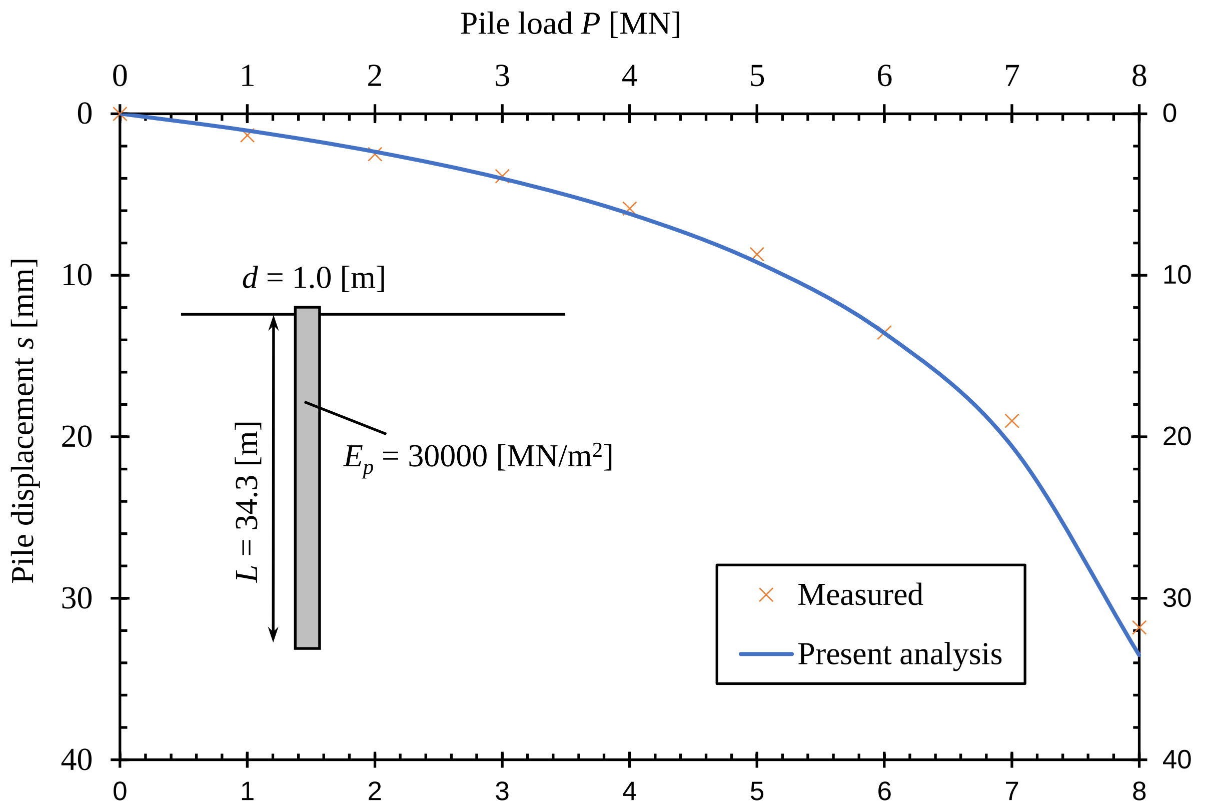

Figure 1.26 Load settlement curve, Case (4).

1.7 References

[1] *Basile, F.* (1999) "Non-linear analysis of pile groups" Vol. 137 (2): 105-115. Doi: https://doi.org/10.1680/gt.1999.370205

[2] *Basu, D., Prezzi, M., Salgado, R.*, and *Chakraborty, T.* (2008) "Settlement analysis of piles with rectangular cross sections in multi-layered soils" Computers and Geotechnics, Vol. 35 (4): 563-575. Doi: https://doi.org/10.1016/j.compgeo.2007.09.001

[3] *Baz, O.* (1987) "Plates on nonlinear subgrade," M. Sc. Thesis, Mansoura University, Mansoura, Egypt.

[4] *Butterfield, R.* and *Banerjee, P. K.* (1971) "The Elastic Analysis of Compressible Piles and Pile Groups" Vol. 21 (1): 43-60. Doi: https://doi.org/10.1680/geot.1971.21.1.43

[5] *De Sanctis, L., Russo, G.*, and *Viggiani, C.* (2002) "Piled Raft On Layered Soils" presented at the Proceedings of the ninth international conference on piling and deep foundations, Nice.

[6] *El Gendy, M.* (1999): An iterative procedure for foundation-superstructure interaction problem.

[7] *El Gendy, M.* (2007) "Formulation of a composed coefficient technique for analyzing large piled raft" Ain Shams Engineering Journal, Vol. 42 (1): 29-56.

[8] *EL Gendy, M.* and *El Gendy, A.* (2021), Analysis and design of raft and piled Raft-Program ELPLA, GEOTEC Software Inc., Canada.

[9] *Fleming, W.* (1992) "A new method for signle pile settlement prediction and analysis" Vol. 42 (3): 411-425. Doi: https://doi.org/10.1680/geot.1992.42.3.411

[10] *Hasnien, M.* (1993) "Finite element analysis of mat resting on nonlinear elastic medium," M. Sc. Thesis, Ain Shams University, Cairo, Egypt.

[11] *Lee, C. Y.* (1991) "Discrete layer analysis of axially loaded piles and pile groups" Computers and Geotechnics, Article Vol. 11 (4): 295-313. Doi: https://doi.org/10.1016/0266-352X(91)90014-7

[12] *Mandolini, A.* and *Viggiani, C.* (1997) "Settlement of piled foundations" Vol. 47 (4): 791-816. Doi: https://doi.org/10.1680/geot.1997.47.4.791

[13] *Mindlin, R. D.* (1936) "Force at a Point in the Interior of a Semi-Infinite Solid" Physics, Vol. 7 (5): 195-202. Doi: https://doi.org/10.1063/1.1745385

[14] *Poulos, H. G.* (1968) "Analysis of the Settlement of Pile Groups" Vol. 18 (4): 449-471. Doi: https://doi.org/10.1680/geot.1968.18.4.449

[15] *Poulos, H. G.* (1979) "Settlement of Single Piles in Nonhomogeneous Soil" Journal of the Geotechnical Engineering Division, Vol. 105 (5): 627-641.

[16] *Poulos, H. G.* and *Davis, E. H.* (1968) "The Settlement Behaviour of Single Axially Loaded Incompressible Piles and Piers" Géotechnique, Vol. 18 (3): 351-371. Doi: https://doi.org/10.1680/geot.1968.18.3.351

[17] *Russo, G.* (1998) "Numerical analysis of piled rafts" International Journal for Numerical and Analytical Methods in Geomechanics, Vol. 22 (6): 477-493. Doi: https://doi.org/10.1002/(SICI)1096-9853(199806)22:6%3C477::AID-NAG931%3E3.0.CO;2-H

[18] *Seo, H.* and *Prezzi, M.* (2007) "Analytical solutions for a vertically loaded pile in multilayered soil" Geomechanics and Geoengineering, Vol. 2 (1): 51-60. Doi: https://doi.org/10.1080/17486020601099380

[19] *Small, J. C.* and *Lee, C. Y.* (1992) "The Analysis of Axially Loaded Piles in Layered or Non-Homogeneous Soils" presented at the 6th Australia - New Zealand Conference on Geomechanics, Christchurch.

[20] *Winkler, E.* (1867) "Die Lehre von der Elastizität und Festigkeit". Dominicus, Prag.

[21] *Yamashita, K., Tomono, M.,* and *Kakurai, M.* (1987) "A Method for Estimating Immediate Settlement of Piles and Pile Groups" Soils and Foundations, Vol. 27 (1): 61-76.
Doi: https://doi.org/10.3208/sandf1972.27.61